

# Analytical approximations to the dynamics of an array of coupled DC SQUIDS

Susan Berggren<sup>1,a</sup> and Antonio Palacios<sup>2</sup>

<sup>1</sup> SPAWAR Systems Center Pacific, 53560 Hull St., San Diego, CA 92152, USA

<sup>2</sup> Nonlinear Dynamical Systems Group, Department of Mathematics, San Diego State University, 5500 Campanile Dr., San Diego, CA 92182, USA

Received 28 January 2014 / Received in final form 5 March 2014

Published online (Inserted Later) – © EDP Sciences, Società Italiana di Fisica, Springer-Verlag 2014

**Abstract.** Coupled dynamical systems that operate near the onset of a bifurcation can lead, under certain conditions, to strong signal amplification effects. Over the past years we have studied this generic feature on a wide range of systems, including: magnetic and electric fields sensors, gyroscopic devices, and arrays of loops of superconducting quantum interference devices, also known as SQUIDS. In this work, we consider an array of SQUID loops connected in series as a case study to derive asymptotic analytical approximations to the exact solutions through perturbation analysis. Two approaches are considered. First, a straightforward expansion in which the non-linear parameter related to the inductance of the DC SQUID is treated as the small perturbation parameter. Second, a more accurate procedure that considers the SQUID phase dynamics as non-uniform motion on a circle. This second procedure is readily extended to the series array and it could serve as a mathematical framework to find approximate solutions to related complex systems with high-dimensionality. To the best of our knowledge, an approximate analytical solutions to an array of SQUIDS has not been reported yet in the literature.

## 1 Introduction

Superconductive materials have the unique property that they lose all resistance to electric current when cooled below a critical temperature [1–3]. When Heike Kamerlingh Onnes and his team at a Leiden University laboratory cooled mercury to 3 K in 1911 he discovered this phenomenon. Fifty-one years after the discovery of superconductivity a thin layer of insulating material was placed separating two superconductors, which was named a Josephson junction. The Josephson junction takes advantage of the phenomenon of quantum tunneling, which occurs when electrons are able to pass through an insulating material under an external magnetic field [4]. Then the direct current (DC) superconducting quantum interference device (SQUID) was invented in 1964 [5] soon after B.D. Josephson postulated the Josephson effect. A SQUID consists of a tiny loop (around 10 by 10  $\mu\text{m}^2$ ) of superconducting material into which one incorporates Josephson junctions. The DC SQUID has two Josephson junctions placed in parallel and it combines the phenomena of flux quantization and Josephson tunneling. The flux contained in a closed superconducting loop is quantized in units of the

flux quantum, which has been predicted theoretically [6] and observed experimentally [7,8]. The flux quantum is  $\Phi_0 \equiv \frac{h}{2e} \approx 2.07 \times 10^{-15}$ , where  $h$  is Planck's constant and  $2e$  is the charge on the Cooper pair.

The Direct Current (DC) SQUID is one of the most sensitive magnetic field devices and it is used in the medical field in areas such as magnetic resonance imaging (MRI), magnetoencephalography (measurements of neural activity inside a brain), magnetogastrography (stomach imaging), and magnetocardiography (heart imaging) [9–17]. In the past 100 years, MRI, used in the medical field to take images of the interior of the human body, has been the main application of superconductivity which has found widespread success. In recent years, arrays of coupled DC SQUIDS have been considered as a general mechanism for improving signal detection and amplification [18–21]. The arrays can yield comparable improvements in signal output, relative to background noise, over those of a single device [18,22,23].

In an array configuration of SQUIDS each loop contains two Josephson junctions, i.e., a standard DC SQUID. Using non-uniformly distributed SQUIDS loop areas in the array exhibits a magnetic field dependent average voltage response  $\langle V(x_e) \rangle$ , where  $x_e$  denotes an external magnetic field normalized by the quantum flux, which has

<sup>a</sup> e-mail: susan.berggren@navy.mil

a pronounced single peak with a large voltage swing at zero external magnetic field, i.e,  $x_e = 0$ . The potential high dynamic range and linearity of the anti-peak voltage response render the array an ideal detector of absolute strength of external magnetic fields, so these arrays are also commonly known as Superconducting Quantum Interference Filters (SQIFs). Since the first time it was theoretically proposed [24,25] and experimentally demonstrated [26–28], the SQIF concept has been investigated and exploited by a continuously growing number of groups with respect to its basic properties [29–31] and its suitability in various fields of application, like magnetometry [32–37] and rf electronics [38–45].

Improving the linearity of the average voltage response is critical for developing advanced technologies, including: low noise amplifier (LNA), which can increase link margins and affect an entire communication system [46–51]; Unmanned Aerial Vehicles (UAVs), where size, weight and power are limited; electrically small antennas, which can provide acceptable gain [40,45,52–54]; and land mine detection [55]. A standard approach to improve linearity and dynamic range of a SQIF device employs electronic feedback. This approach, unfortunately, tends to limit the frequency response of the system [56]. In order to obtain large signal frequency response, feedback cannot be used and, therefore, series arrays of identical DC SQUIDs have also been studied [57], however, the single anti-peak response is more desirable.

An iterative method in which a small parameter is used to create an asymptotic expansion for the solution of a system of equations is known as a perturbation analysis. A perturbation analysis is important because it can provide an approximate analytical solution for a system, which is not directly solvable. In turn, this approximate analytical solution can be used to conduct computer simulations in a more timely fashion. While attempts of a perturbation analysis of the dynamics of a single DC SQUID have been performed previously [58,59], a full analytical solution to the average voltage response of an array of DC SQUIDs had not been successfully completed. In this paper, we perform a perturbation analysis on the single DC SQUID phase equations in two different ways. First, we seek a straight forward expansion using the non-linear parameter related to the inductance,  $\beta$ , of the DC SQUID as the perturbation parameter [58,60–62]. Second, we employ a procedure that preprocesses the differential equations into a system that represents non-uniform motion on a circle [59,62–67]. This second procedure is much more complex but it is also much more accurate. Then we extend the second approach to find approximate analytical solutions to the series coupled array of SQUIDs.

## 2 Background

A single DC SQUID has two Josephson junctions arranged in parallel, connected with superconducting material, see Figure 1. In order to model the dynamics of this system there are some assumptions that need to be considered.

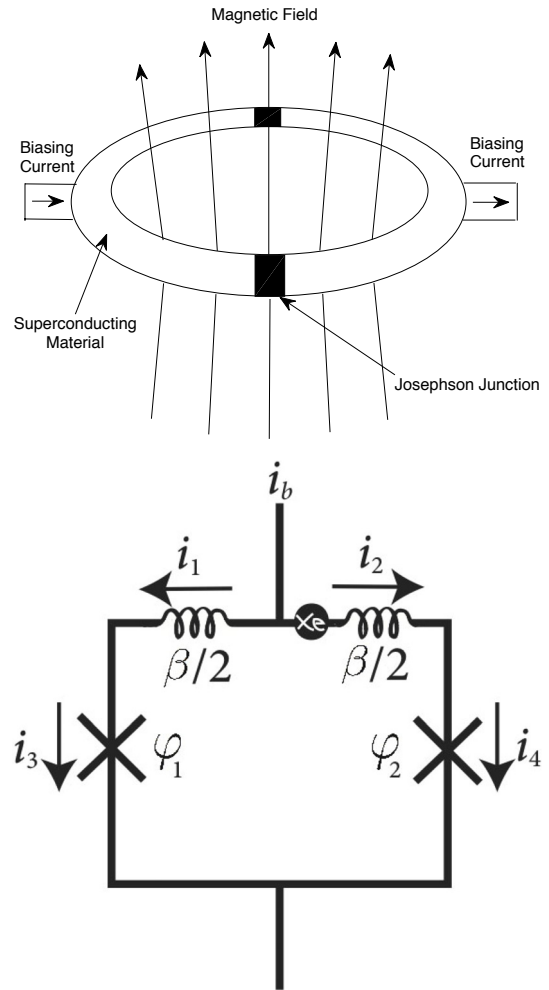


**Fig. 1.** Schematic diagram of a single DC SQUID with the magnetic field shown (top) and the currents listed (bottom).

One assumption is that the Josephson junctions are symmetric. The voltage measured across the two Josephson junctions is usually the state “output”, however, it is the circulating current  $I_s$ , experimentally equivalent to the “shielding flux”, which is used as the output variable of interest.

In the presence of an external magnetic flux  $\Phi_e$ , one obtains a loop flux consisting of the (geometrical) component  $\Phi_e$  together with a contribution arising from the induced circulating or shielding current  $I_s$  that tends to screen the applied flux

$$\Phi = \Phi_e + LI_s, \quad (1)$$

where  $L$  is the loop inductance. For a Josephson junction that is over-damped the wave-function is single-valued around the SQUID loop, leading to the phase continuity condition

$$\varphi_2 - \varphi_1 = 2\pi n - 2\pi \frac{\Phi}{\Phi_0}, \quad (2)$$

where  $\varphi_1$  and  $\varphi_2$  are the phases across each of the Josephson junctions,  $\Phi_0 \equiv \frac{h}{2e}$  is the flux quantum and  $n$  is an integer representing the eigenstate of the flux in

the SQUID.  $n$  can be set to zero since the flux contained in a closed superconducting loop is quantized in units of the flux quantum, and combine equations (1) and (2) to find

$$\beta \frac{I_s}{I_0} = \varphi_1 - \varphi_2 - 2\pi \frac{\Phi_e}{\Phi_0}, \quad (3)$$

where  $\beta = 2\pi \frac{LI_0}{\Phi_0}$  is the nonlinear parameter, and  $I_0$  is the critical current of the Josephson junctions. To simplify the equations slightly from here on  $2\pi \frac{\Phi_e}{\Phi_0}$  will be written as  $\varphi_e$ .

Using a resistively shunted junction (RSJ) model of the Josephson junction to reduce hysteresis in the output with a lumped circuit representation [68], the currents in the two arms of the SQUID can be modeled. This method uses the Josephson relations,  $\frac{d\varphi_i}{dt} = \frac{2e}{\hbar} V_i$  for  $i = 1, 2$ , which link the voltage and the quantum phase difference across the junction  $i$ , with Planck's constant  $\hbar$ , the voltage in the  $i$ th junction  $V_i$ , and the charge of an electron  $e$ . The resulting model is:

$$\begin{aligned} \frac{1}{\omega} \frac{d\varphi_1}{dt} &= \frac{I_b}{2} - I_s - I_0 \sin \varphi_1 \\ \frac{1}{\omega} \frac{d\varphi_2}{dt} &= \frac{I_b}{2} + I_s - I_0 \sin \varphi_2, \end{aligned} \quad (4)$$

where  $\omega \equiv \frac{2eR_N}{\hbar}$  is the SQUID time constant, and  $I_b$  is the bias current. The parameter  $R_N$  in  $\omega$  is the normal state resistance of the Josephson junctions. In experiments [69] the DC bias current and flux are externally controllable. Dividing equation (4) by  $I_0$  results in

$$\begin{aligned} \frac{1}{\omega_c} \frac{d\varphi_1}{dt} &= J - \frac{I_s}{I_0} - \sin \varphi_1 \\ \frac{1}{\omega_c} \frac{d\varphi_2}{dt} &= J + \frac{I_s}{I_0} - \sin \varphi_2, \end{aligned}$$

where  $\omega_c = \omega I_0$  is a rescaling of the time constant, and  $J = \frac{I_b}{2I_0}$  is a dimensionless quantity known as the normalized bias flux. For the computational modeling, both the parameters  $\omega_c$  and  $I_0$  are set to one. The final form of the model is obtained by substituting  $\frac{I_s}{I_0}$  from equation (3) to yield, after some simplification, the following expressions for the phase dynamics

$$\begin{aligned} \dot{\varphi}_1 &= J - \frac{1}{\beta}(\varphi_1 - \varphi_2 - \varphi_e) - \sin \varphi_1 \\ \dot{\varphi}_2 &= J + \frac{1}{\beta}(\varphi_1 - \varphi_2 - \varphi_e) - \sin \varphi_2, \end{aligned} \quad (5)$$

where the dots denote the time differentiation with normalized time  $\tau = \omega_c t = \frac{2eI_0R_N}{\hbar} t$  of the phases across the Josephson junctions  $\varphi_1$  and  $\varphi_2$ . The variable  $\varphi_e = 2\pi\alpha x_e$ , where  $x_e$  is the normalized external magnetic flux, and  $\alpha$  is related to the size of the SQUID. We use the approximate assumption that  $\alpha = \beta$ .

The output of the DC SQUID we want to reproduce analytically through the perturbation analysis is the average voltage response. The average voltage,  $\langle V \rangle$ , of a SQUID at a point in  $x_e$  is the mean value of the voltage over time. Between 101 and 501 points in  $x_e$  are calculated

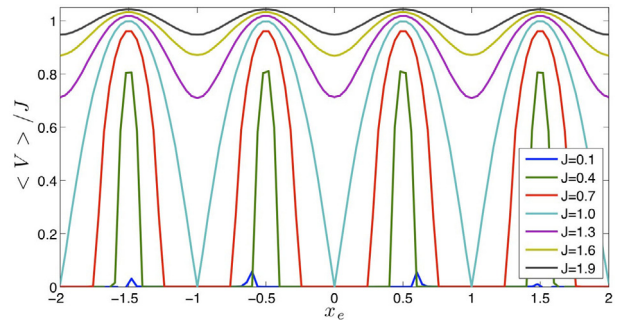


**Fig. 2.** Average voltage output of a DC SQUID for  $J$  values between 0.1 and 1.9 for  $\beta = 1.0$  and  $x_e$  between  $-2$  and  $2$ .

depending on how detailed the image needs to be and the range of  $x_e$ . An example of the average voltage response of a single SQUID over a range of values of  $J$  is shown in Figure 2. The average voltage response was divided by  $J$  so that all the plots are on the same scale and are comparable. When  $J < 1$  there are numerous values of  $x_e$  for which  $\langle V \rangle$  is zero. As  $J$  becomes larger and larger beyond one the voltage swing of the average voltage response decreases drastically. An ideal average voltage response has a large voltage swing and no values for which  $\langle V \rangle = 0$ . This is the reason a number close to one, but slightly larger, is chosen for the value of  $J$ .

### 3 Single DC SQUID perturbation analysis

The perturbation analysis of the single DC SQUID begins with the phase equations in equation (5). We will investigate two approaches to find an analytical solution. The first of which is the straightforward expansion using  $\beta$  as the perturbation parameter.

#### 3.1 Straightforward expansion

Equation (5) is reorganized using the sum and difference formulas,  $\Sigma = \frac{\varphi_1 + \varphi_2}{2}$  and  $\delta = \frac{\varphi_1 - \varphi_2}{2}$ , respectively, to become

$$\begin{aligned} \frac{d\Sigma}{d\tau} &= J - \sin \Sigma \cos \delta \\ \frac{d\delta}{d\tau} &= -\frac{2}{\beta} \delta + \frac{2}{\beta} \pi \alpha x_e - \sin \delta \cos \Sigma. \end{aligned} \quad (6)$$

If a time shift  $\nu = \frac{2}{\beta} \tau$  is defined such that  $\frac{d\delta}{d\tau} = \frac{d\delta}{d\nu} \frac{d\nu}{d\tau} = \frac{2}{\beta} \frac{d\delta}{d\nu}$  then the fast and slow time scales in the system of equations in equation (6) are given by  $\frac{2\tau}{\beta}$  and  $\tau$ , respectively.  $\Sigma$  and  $\delta$  are expanded in terms of the parameter  $\beta$  in  $\tau$  and  $\nu$  as follows:

$$\begin{aligned} \Sigma(\beta, \tau) &\approx \Sigma_0(\tau) + \beta \Sigma_1(\tau) + \dots \\ \delta(\beta, \nu) &\approx \delta_0(\nu) + \beta \delta_1(\nu) + \dots \end{aligned} \quad (7)$$

Substituting the expansions in equation (7) into equation (6) and multiplying the second equation by  $\frac{\beta}{2}$  yields

$$\begin{aligned} \frac{d\Sigma_0(\tau)}{d\tau} + \beta \frac{d\Sigma_1(\tau)}{d\tau} + \dots &= J - \cos(\delta_0(\nu) + \beta\delta_1(\nu) + \dots) \\ &\quad \times \sin(\Sigma_0(\tau) + \beta\Sigma_1(\tau) + \dots) \\ \frac{d\delta_0(\nu)}{d\nu} + \beta \frac{d\delta_1(\nu)}{d\nu} + \dots &= -\delta_0(\nu) - \beta\delta_1(\nu) - \dots + \pi\alpha x_e \\ &\quad - \frac{\beta}{2} \sin(\delta_0(\nu) + \beta\delta_1(\nu) + \dots) \\ &\quad \times \cos(\Sigma_0(\tau) + \beta\Sigma_1(\tau) + \dots). \end{aligned}$$

Using Taylor expansions for cosine and sine and grouping like orders of  $\beta$ , the equations become

$$\begin{aligned} \frac{d\Sigma_0(\tau)}{d\tau} + \beta \frac{d\Sigma_1(\tau)}{d\tau} &= J + \sin \Sigma_0(\tau) \sin \delta_0(\nu) \beta \delta_1(\nu) \\ &\quad - \cos \Sigma_0(\tau) \beta \Sigma_1(\tau) \cos \delta_0(\nu) \\ &\quad - \sin \Sigma_0(\tau) \cos \delta_0(\nu) + \mathcal{O}(\beta^2) \\ \frac{d\delta_0(\nu)}{d\nu} + \beta \frac{d\delta_1(\nu)}{d\nu} &= -\delta_0(\nu) - \beta \delta_1(\nu) + \pi\alpha x_e \\ &\quad - \frac{\beta}{2} \sin \delta_0(\nu) \cos \Sigma_0(\tau) + \mathcal{O}(\beta^2). \end{aligned} \quad (8)$$

Collecting the coefficients of like powers of  $\beta$  from equation (8) gives the  $\mathcal{O}(\beta^0)$  equations

$$\begin{aligned} \frac{d\Sigma_0(\tau)}{d\tau} &= J - \sin \Sigma_0(\tau) \cos \delta_0(\nu) \\ \frac{d\delta_0(\nu)}{d\nu} &= -\delta_0(\nu) + \pi\alpha x_e, \end{aligned}$$

and the  $\mathcal{O}(\beta^1)$  equations become

$$\begin{aligned} \frac{d\Sigma_1(\tau)}{d\tau} &= \sin \Sigma_0(\tau) \sin \delta_0(\nu) \delta_1(\nu) \\ &\quad - \cos \Sigma_0(\tau) \cos \delta_0(\nu) \Sigma_1(\tau) \\ \frac{d\delta_1(\nu)}{d\nu} &= -\delta_1(\nu) - \frac{1}{2} \sin \delta_0(\nu) \cos \Sigma_0(\tau). \end{aligned}$$

### Perturbation solution

The details of the straightforward perturbation analysis are contained in Appendix A. The asymptotic expansion for approximating the dynamics for a single DC SQUID can be summarized as follows

$$\begin{aligned} \Sigma(\beta, \tau) &\approx \Sigma_0(\tau) + \beta \Sigma_1(\tau) + \dots \\ \delta(\beta, \nu) &\approx \delta_0(\nu) + \beta \delta_1(\nu) + \dots, \end{aligned}$$

where each of the components are

$$\begin{aligned} \delta_0(\nu) &= \pi\alpha x_e \\ \Sigma_0(\tau) &= 2 \arctan \left( a + \sqrt{A} \tan(\Gamma) \right) \\ \delta_1(\nu) &= -\frac{1}{2} \sin \delta_0(\nu) \cos \left( \Sigma_0 \left( \frac{\beta}{2} \nu \right) \right) \\ \Sigma_1(\tau) &= \frac{8\pi \sin(\pi x_e)^2 \left( \tan(\Gamma) + a\sqrt{A} - a^3\sqrt{A} \right)}{\gamma 4A(1 + a^2 + 2a\sqrt{A} \tan(\Gamma) + A \tan(\Gamma)^2)} \\ &\quad + \frac{8\pi \sin(\pi x_e)^2 \left( -2 \arctan(\Gamma) a + a^4 \tan(\Gamma) \right)}{\gamma 4A(1 + a^2 + 2a\sqrt{A} \tan(\Gamma) + A \tan(\Gamma)^2)} \\ &\quad - \frac{\pi \sin(\pi x_e)^2 \ln(1 + a^2 + 2a\sqrt{A} \tan(\Gamma))}{\gamma a^2 \sqrt{A}} \\ &\quad - \frac{-a^2 \tan(\Gamma)^2 + \tan(\Gamma)^2 A}{\gamma a^2 \sqrt{A}} \\ &\quad + \frac{\pi \sin(\pi x_e)^2 \sqrt{A} \ln(1 + \tan(\Gamma)^2)}{\gamma a^2} + C_0, \end{aligned} \quad (9)$$

where

$$C_0 = \int e^{\int -p(\tau) d\tau} \left( \int e^{\int p(\tau) d\tau} q(\tau) d\tau \Big|_{\tau=0} \right)$$

$$\Gamma = \gamma\tau + \arctan(\xi_0)$$

$$a = \frac{\cos \delta_0(\nu)}{J}$$

$$A = 1 - a^2$$

$$\gamma = \frac{1}{2} \sqrt{J^2 - \cos^2 \delta_0(\nu)}$$

$$\xi_0 = \frac{\tan \left( \frac{1}{2} \Sigma_0(0) \right) - a}{\sqrt{1 - a^2}}$$

$$\nu = \frac{2}{\beta} \tau.$$

The solutions for small values of  $\beta$  found from equation (9) fit very well with the solutions obtained from solving the system of differential equations in equation (5) with the Matlab Runge-Kutta numerical solver `ode45`. An example where  $\beta = 0.1$  is shown in Figure 3. On the top the results from the average phase  $\Sigma(\tau)$  are shown and on the bottom the plot for the phase difference  $\delta(\nu)$  is depicted. Both comparison plots show very good agreement with the simulated results. The RMS (Root-Mean-Square) error between the simulated and numerical solutions for  $\Sigma(\tau)$  is  $4.34772 \times 10^{-4}$ . This error measurement is

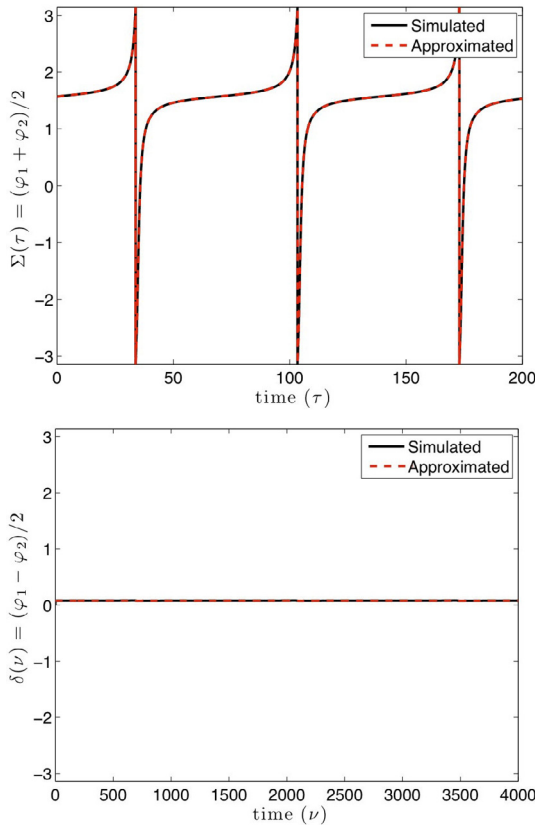


**Fig. 3.** Results of perturbation analysis of a single DC SQUID for small  $\beta$  values, here  $\beta = 0.1$ ,  $x_e = 0.25$ ,  $\alpha = 0.1$ ,  $J = 1.001$ ,  $\Sigma(0) = \frac{\pi}{2}$ . The top plot is  $\Sigma(\tau)$  and the bottom plot is  $\delta(\nu)$ .

calculated as:

$$\text{RMS} = \frac{1}{N} \sqrt{\sum_{k=1}^N (\langle V \rangle_s(k) - \langle V \rangle_a(k))^2},$$

for which  $\langle V \rangle_s$  is the simulated average voltage,  $\langle V \rangle_a$  is the analytical approximation obtained through the perturbation analysis, and  $N$  is the number points in  $x_e$ . The error between the numerical solution and the simulated solution for  $\delta(\nu)$  is  $4.09142 \times 10^{-6}$ .

Once  $\beta$  is increased to the range 0.5 to 1.5 issues with the accuracy of the approximate analytical solutions become more visible. Figure 4 shows the simulated and numerical solutions for  $\beta = 0.5$ . There appears to be a very good agreement between the numerical solution from the perturbation analysis and the simulated results from the code for this value of  $\beta$ . The RMS error between the simulated and numerical solutions for  $\Sigma(\tau)$  is  $4.28130 \times 10^{-3}$ , a full order of magnitude larger than the case where  $\beta = 0.1$ . For  $\delta(\nu)$  it is  $1.32602 \times 10^{-4}$ , two full orders of magnitude larger than the case where  $\beta = 0.1$ .

In Figure 5, the solutions for  $\Sigma(\tau)$  and  $\delta(\nu)$  with parameters  $\beta = 1.0$ ,  $x_e = 0.25$ ,  $\alpha = 0.1$ ,  $J = 1.001$ ,  $\Sigma(0) = \frac{\pi}{2}$  are shown, where top plot is  $\Sigma(\tau)$  and the bottom plot is  $\delta(\nu)$ . For most of the array distributions we are interested in  $\beta = 1.0$  is the midpoint value. The simulated and numerical solutions for this value of  $\beta$  no

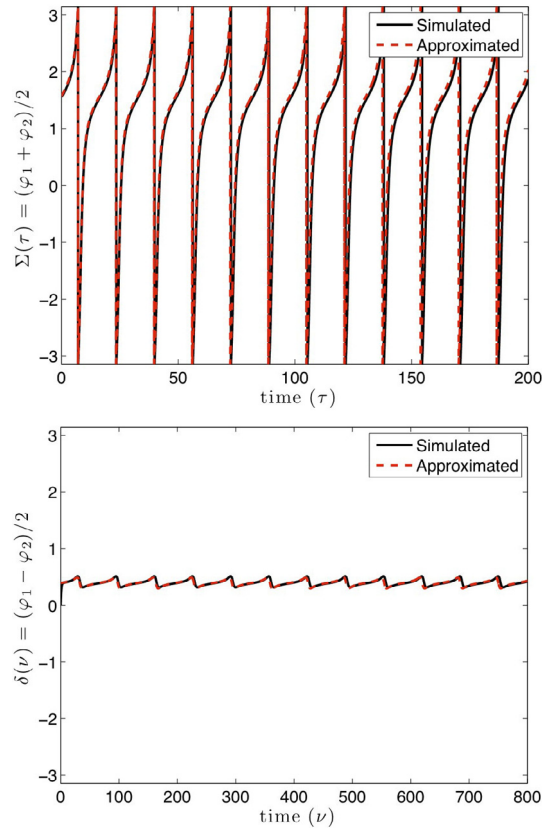


**Fig. 4.** Results of perturbation analysis of a single DC SQUID for  $\beta = 0.5$ ,  $x_e = 0.25$ ,  $\alpha = 0.5$ ,  $J = 1.001$ ,  $\Sigma(0) = \frac{\pi}{2}$ . The top plot is  $\Sigma(\tau)$  and the bottom plot is  $\delta(\nu)$ .

longer match. The RMS error between the simulated and numerical solutions for  $\Sigma(\tau)$  is 0.0101019 and for  $\delta(\nu)$  it is 0.001401005. Both of these error measurements are full orders of magnitude larger than when  $\beta = 0.5$ . Notice that when  $\beta$  increases the shift in time  $\nu = \frac{2}{\beta}\tau$  is no longer slow time scale so that the adiabatic simplification of  $\delta_0(\nu)$  and  $\delta_1(\nu)$  no longer holds, thus the approximation degrades.

The difference between the numerical solutions and the simulated solutions when  $\beta = 1.5$  are much greater than for smaller values of  $\beta$ , see Figure 6. Neither the solution of  $\Sigma(\tau)$  nor that of  $\delta(\nu)$  line up with the simulations. The RMS error between the simulated and numerical solutions for  $\Sigma$  is 0.0112579, larger than it was previously. For  $\delta$  it is 0.00280592, which is double the error value than in the case when  $\beta = 1.0$ . It can be concluded that this form of perturbation analysis is not ideal for numerically estimating the average voltage response of the SQUID arrays.

The average voltage response  $\langle V \rangle$  is calculated by averaging the quantity  $V(\tau) = \frac{\dot{\varphi}_1 + \dot{\varphi}_2}{2} = \dot{\Sigma}$  over a range of  $x_e$  values. Figure 7 shows the comparison of the simulated and numerical results for the average voltage response with  $\beta = 1.0$ ,  $\alpha = 0.1$ ,  $J = 1.001$ ,  $\Sigma(0) = \frac{\pi}{2}$  and  $x_e = [-2, 2]$ . The simulations took 197.49 s to calculate the average voltage response and the analytical solution took 15.07 s. The speedup achieved by using the analytical solution over the integrations is 13.10, which is significant.

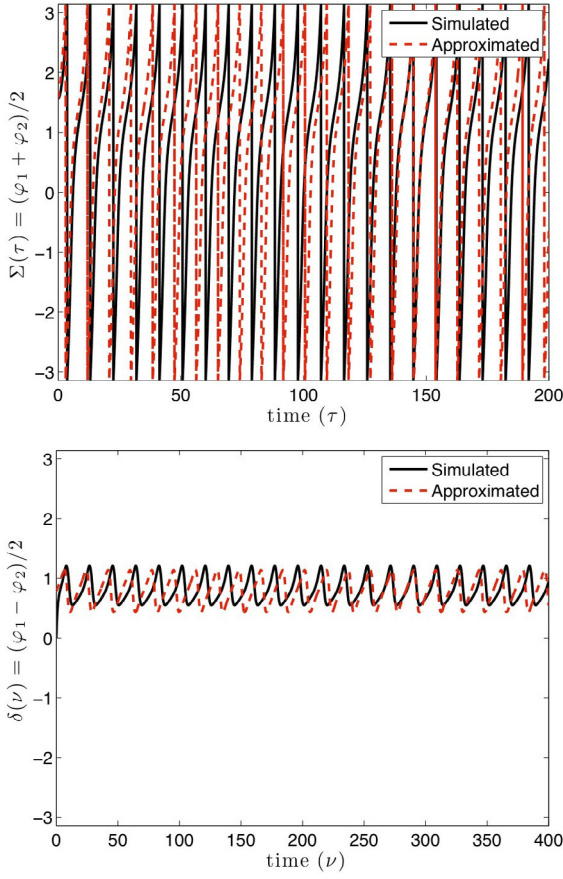


**Fig. 5.** Results of perturbation analysis of a single DC SQUID for  $\beta = 1.0$ ,  $x_e = 0.25$ ,  $\alpha = 1.0$ ,  $J = 1.001$ ,  $\Sigma(0) = \frac{\pi}{2}$ . The top plot is  $\Sigma(\tau)$  and the bottom plot is  $\delta(\nu)$ .

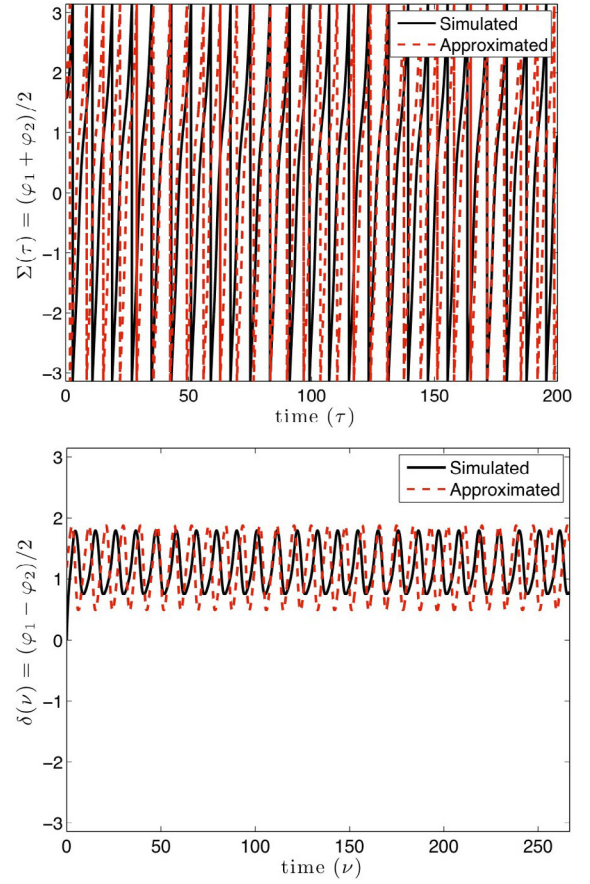


**Fig. 6.** Results of perturbation analysis of a single DC SQUID for  $\beta = 1.5$ ,  $x_e = 0.25$ ,  $\alpha = 1.5$ ,  $J = 1.001$ ,  $\Sigma(0) = \frac{\pi}{2}$ . The top plot is  $\Sigma(\tau)$  and the bottom plot is  $\delta(\nu)$ .

The numerical results approximated by the perturbation analysis overestimate the simulated results at almost every point in  $x_e$  and result in an RMS error of 0.00388943.

It can be concluded that the numerical solutions resulting from the straightforward asymptotic expansion, which uses  $\beta$  as the perturbation parameter, are not very accurate for the range of parameters within the context of arrays of SQUIDs. An alternate way to approximate the analytical solution is needed in order to extend the analysis to coupled arrays and get more accurate results.

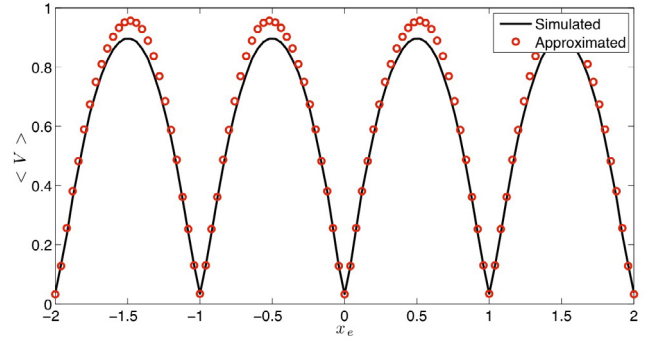


**Fig. 7.** Average voltage response comparison of simulated and numerical results of a single DC SQUID for  $\beta = 1.0$ ,  $\alpha = 1.0$ ,  $J = 1.001$ ,  $\Sigma(0) = \frac{\pi}{2}$  and  $x_e \in [-2, 2]$ .

### 3.2 Hybrid approach: non-uniform oscillators

The second approach that we explore in this work is a perturbation analysis around the parameter  $\varepsilon = (a - a_0)$  that results from manipulation of the phase equations. This method should be more accurate over the range of  $\beta$  values used in the computational analysis. Finding an approximate solution to the single SQUID phase equations begins by applying the transformations  $\Sigma = \frac{\varphi_1 + \varphi_2}{2}$  and

$\delta = \varphi_1 - \varphi_2 - 2\pi\alpha x_e$  to equation (5), which yields

$$\begin{aligned}\dot{\Sigma} &= J - \sin \Sigma \cos \left( \frac{\delta + 2\pi\alpha x_e}{2} \right) \\ \dot{\delta} &= -\frac{2}{\beta}\delta - 2 \cos \Sigma \sin \left( \frac{\delta + 2\pi\alpha x_e}{2} \right).\end{aligned}$$

Letting  $\theta = \Sigma - \frac{\pi}{2}$  and recalling that  $\sin(A + \frac{\pi}{2}) = \cos A$  and  $\cos(A + \frac{\pi}{2}) = -\sin A$ , the following expressions are

arrived at

$$\begin{aligned}\dot{\theta} &= J - \cos \theta \cos \left( \frac{\delta + 2\pi\alpha x_e}{2} \right) \\ \dot{\delta} &= -\frac{2}{\beta}\delta + 2 \sin \theta \sin \left( \frac{\delta + 2\pi\alpha x_e}{2} \right).\end{aligned}$$

The goal is to write the first equation in the form of non-uniform motion on a circle. If  $\bar{\tau} = J\tau$ , then  $\frac{d\theta}{d\tau} = \frac{d\theta}{d\bar{\tau}} \frac{d\bar{\tau}}{d\tau} = J \frac{d\theta}{d\bar{\tau}}$  and by reorganizing the equations become

$$\begin{aligned}\theta' &= 1 + a \cos \theta \\ \dot{\delta} &= -\frac{2}{\beta}\delta + 2 \sin \theta \sin \left( \frac{\delta + 2\pi\alpha x_e}{2} \right),\end{aligned}\quad (10)$$

where  $a = -\frac{1}{J} \cos\left(\frac{\delta+2\pi\alpha x_e}{2}\right)$  and  $\theta' = \frac{d\theta}{d\bar{\tau}}$ . Rewriting  $\theta'$  as:

$$\theta' = 1 + a_0 \cos \theta + (a - a_0) \cos \theta,$$

where  $a_0 = -\frac{1}{J} \cos\left(\frac{\langle\delta\rangle+2\pi\alpha x_e}{2}\right)$  in which  $\langle\delta\rangle = \frac{1}{T} \int_0^T \delta(\tau) d\tau$  for which  $T$  is the period of oscillations in  $\delta$ . Setting  $(a - a_0) = \varepsilon$  results in

$$\theta' = 1 + a_0 \cos \theta + \varepsilon \cos \theta. \quad (11)$$

An approximate solution to  $\theta$  and  $\delta$  are sought in the form

$$\begin{aligned}\theta(\tau) &= \theta_0(\tau) + \varepsilon\theta_1(\tau) + \dots \\ \delta(\tau) &= \delta_0(\tau) + \varepsilon\delta_1(\tau) + \dots\end{aligned}\quad (12)$$

Substituting equation (12) into equation (11) and the second equation in equation (10), and expanding up to  $\mathcal{O}(\varepsilon^0)$  gives

$$\begin{aligned}\theta'_0 &= 1 + a_0 \cos \theta_0 \\ \dot{\delta}_0 &= -\frac{2}{\beta}\delta_0 + 2 \sin \theta_0 \sin \left( \frac{\delta_0 + 2\pi\alpha x_e}{2} \right).\end{aligned}\quad (13)$$

### Perturbation solution

Appendix B contains the details of the perturbation analysis that solves equation (13). The asymptotic expansion for approximating the dynamics for a single DC SQUID determined from the hybrid approach can be summarized as follows:

$$\Sigma(\varepsilon, \tau) \approx \frac{\pi}{2} + 2 \tan^{-1} \left[ b^{-1} \tan \left( \frac{\phi(\tau)}{2} \right) \right]$$

$$\delta(\varepsilon, \tau) \approx K \frac{c \sin(\phi(\tau)) - \cos \phi(\tau)}{1 - a_0 \cos \phi(\tau)},$$

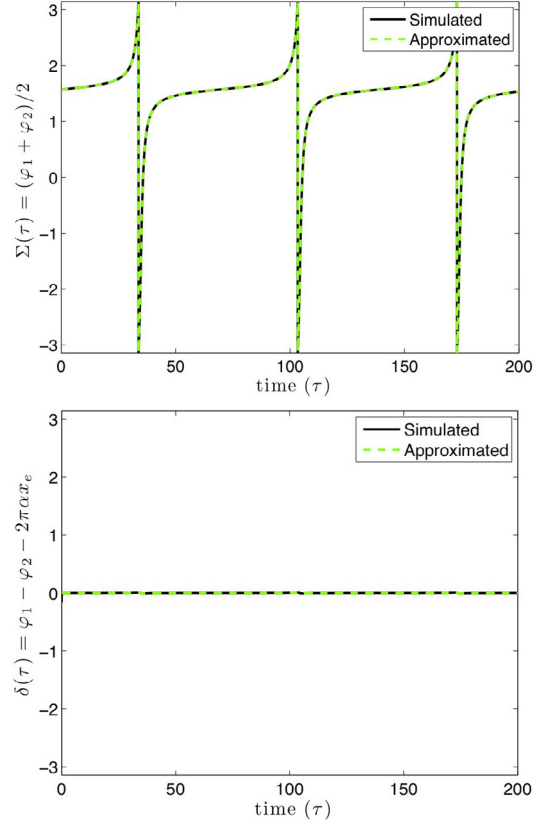


**Fig. 8.** The results of the perturbation analysis of a single DC SQUID for  $\Sigma(\tau)$  (top) and  $\delta(\tau)$  (bottom) compared with the simulated results where  $\beta = 0.1$ ,  $x_e = 0.25$ ,  $\alpha = 0.1$ ,  $J = 1.001$ ,  $\Sigma(0) = \frac{\pi}{2}$ .

where

$$\begin{aligned}b &= \sqrt{\frac{1 - a_0}{1 + a_0}} \\ a_0 &= -\frac{1}{J} \cos \left( \frac{\langle\delta\rangle + 2\pi\alpha x_e}{2} \right) \\ c &= \frac{2}{\beta\omega_0} \\ K &= \frac{2 \sin(\pi\alpha x_e)}{J(1 + c^2)} \\ \phi(\tau) &= (\omega_0 + \Delta\omega)\tau \\ \omega_0 &= J\sqrt{1 - a_0^2} \\ \Delta\omega &= \frac{\sin(\pi\alpha x_e)K}{2} \frac{\sqrt{1 - a_0^2} - 1}{a_0^2} \\ &\quad + \frac{\cos(\pi\alpha x_e)K^2 (a_0^2 - 2 - c^2(3a_0^2 - 2))\sqrt{1 - a_0^2}}{16 a_0^3(1 - a_0^2)} \\ &\quad - \frac{\cos(\pi\alpha x_e)K^2 c^2(2a_0^4 - 4a_0^2 + 2) + 2 - 2a_0^2}{16 a_0^3(1 - a_0^2)}.\end{aligned}$$

To study how well the analytical solution from the hybrid perturbation analysis fits the simulated solutions  $\Sigma(\tau)$  and  $\delta_0(\tau)$  are plotted together. In particular, Figure 8

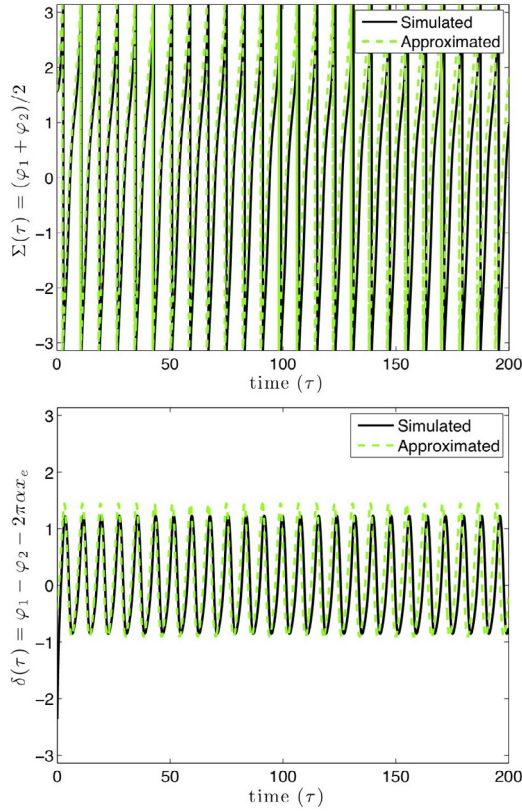
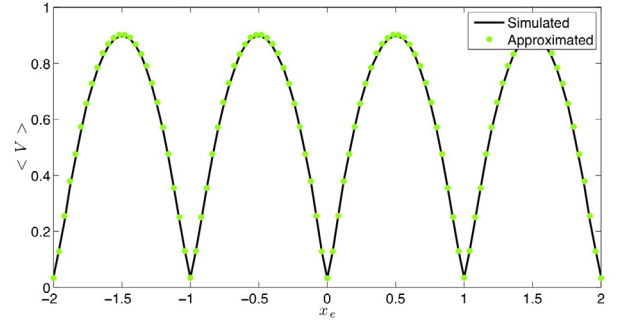


**Fig. 9.** The results of the perturbation analysis of a single DC SQUID for  $\Sigma(\tau)$  (top) and  $\delta(\tau)$  (bottom) compared with the simulated results where  $\beta = 1.5$ ,  $x_e = 0.25$ ,  $\alpha = 1.5$ ,  $J = 1.001$ ,  $\Sigma(0) = \frac{\pi}{2}$ .

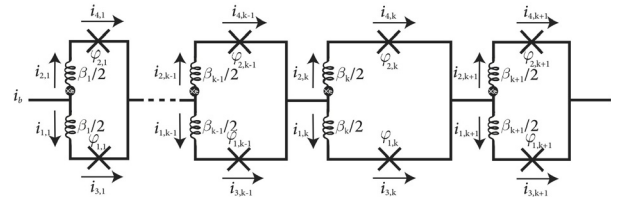
shows the results for  $\beta = 0.1$ . As in the case of the straightforward approach, the numerical and simulated solution are almost identical. The RMS error between the simulated and numerical solutions for  $\Sigma$  is  $2.24046 \times 10^{-4}$  while for  $\delta(\tau)$  it is  $3.96683 \times 10^{-6}$ . Both error values are of the same magnitude as those of the straightforward expansion.

Figure 9 shows a similar comparison for  $\beta = 1.5$ . The approximated solution for  $\Sigma(\tau)$  slightly overshoots the simulated solution, but this solution is far more accurate than the one in the straightforward approach, recall Figure 6. The RMS error between the simulated and numerical solutions for  $\Sigma(\tau)$  is 0.0044326 while for  $\delta(\tau)$  it is 0.0015072. The error for  $\Sigma(\tau)$  is an order of magnitude less and the error for  $\delta(\tau)$  is half the magnitude when compared with the solutions from the straightforward expansion. Since the perturbation analysis does not employ  $\beta$  as the small parameter, the issue of the solution not being accurate for large values of  $\beta$  is no longer a problem. Furthermore, since the relevant values of  $\beta$  are in the range  $[0.5 : 1.5]$ , the hybrid approach perturbation analysis can be deemed to be superior to the straightforward approach.

In Figure 10 the average voltage response of a single SQUID is calculated with  $\beta = 1.0$ ,  $\alpha = 0.1$ ,  $J = 1.001$ ,  $\Sigma(0) = \frac{\pi}{2}$  and  $x_e = [-2, 2]$ . The simulations took 197.49 s to calculate the average voltage response and the ana-



**Fig. 10.** The average voltage response of a single DC SQUID calculated from the perturbation analysis compared with the simulated results for  $\beta = 1.0$  with  $x_e = [-2, 2]$ ,  $\alpha = 1.0$ ,  $J = 1.001$ ,  $\Sigma(0) = \frac{\pi}{2}$ .



**Fig. 11.** Circuit representation of a series coupled SQUID array, where  $(i_b, i_{1,k}, i_{2,k}, i_{3,k}, i_{4,k})$  represent the normalized currents,  $(\varphi_{1,k}, \varphi_{2,k})$  are the phases across the Josephson junctions, and  $(\beta_k/2)$  are the parameters related to the inductance values.

lytical solution took only 1.77 s. The speedup achieved by using the analytical solution over the integrations is 111.58, which is even greater than for the straightforward approach. Also, here the perturbation solution overestimates the simulated results slightly but to a much less extent than the results from the straightforward expansion (recall Fig. 7). There is an RMS error between the numerical and simulated values for the average voltage response of 0.0010147. This is a quarter of the error when compared with the average voltage response of the straightforward approach.

#### 4 Arrays of DC SQUIDs coupled in series

We now extend perturbation analysis to arrays of SQUIDs coupled in series. This type of array consists of individual DC SQUIDs, which are connected to each other without sharing junctions or sides, see Figure 11. The bias current is fed to each of the SQUIDs in the array, and the output is measured at each of the Josephson junctions with the control lines. Each SQUID has a different area designated by the different loop sizes. The circuit representation of  $N$  SQUIDs coupled in series can be seen in Figure 11. In the circuit  $(i_b, i_{1,k}, i_{2,k}, i_{3,k}, i_{4,k})$  represent the normalized currents,  $(\varphi_{1,k}, \varphi_{2,k})$  are the phases across the Josephson junctions,  $\beta_k/2$  are the parameters related to the inductance values, with  $k = 1, \dots, N$ , and  $x_e$  are the points in the array where the contributions from external fields are included.

#### 4.1 Phase equations

The phase equations are derived in a similar fashion to the single DC SQUID, with the additional term included for the nearest neighbor coupling with strength  $M$ :

$$\begin{aligned}
\dot{\varphi}_{1,1} &= J - \sin \varphi_{1,1} - \frac{1}{\beta_1} \left( \varphi_{1,1} - \varphi_{2,1} - \varphi_{e,1} \right. \\
&\quad \left. - \frac{M}{\beta_2} (\varphi_{1,2} - \varphi_{2,2} - \varphi_{e,2}) \right) \\
\dot{\varphi}_{2,1} &= J - \sin \varphi_{2,1} + \frac{1}{\beta_1} \left( \varphi_{1,1} - \varphi_{2,1} - \varphi_{e,1} \right. \\
&\quad \left. - \frac{M}{\beta_2} (\varphi_{1,2} - \varphi_{2,2} - \varphi_{e,2}) \right) \\
\dot{\varphi}_{1,k} &= J - \sin \varphi_{1,k} - \frac{1}{\beta_k} \left( \varphi_{1,k} - \varphi_{2,k} - \varphi_{e,k} \right. \\
&\quad - \frac{M}{\beta_{k+1}} (\varphi_{1,k+1} - \varphi_{2,k+1} - \varphi_{e,k+1}) \\
&\quad \left. - \frac{M}{\beta_{k-1}} (\varphi_{1,k-1} - \varphi_{2,k-1} - \varphi_{e,k-1}) \right) \\
\dot{\varphi}_{2,k} &= J - \sin \varphi_{2,k} + \frac{1}{\beta_k} \left( \varphi_{1,k} - \varphi_{2,k} - \varphi_{e,k} \right. \\
&\quad - \frac{M}{\beta_{k+1}} (\varphi_{1,k+1} - \varphi_{2,k+1} - \varphi_{e,k+1}) \\
&\quad \left. - \frac{M}{\beta_{k-1}} (\varphi_{1,k-1} - \varphi_{2,k-1} - \varphi_{e,k-1}) \right) \\
\dot{\varphi}_{1,N} &= J - \sin \varphi_{1,N} - \frac{1}{\beta_N} \left( \varphi_{1,N} - \varphi_{2,N} - \varphi_{e,N} \right. \\
&\quad \left. - \frac{M}{\beta_{N-1}} (\varphi_{1,N-1} - \varphi_{2,N-1} - \varphi_{e,N-1}) \right) \\
\dot{\varphi}_{2,N} &= J - \sin \varphi_{2,N} + \frac{1}{\beta_N} \left( \varphi_{1,N} - \varphi_{2,N} - \varphi_{e,N} \right. \\
&\quad \left. - \frac{M}{\beta_{N-1}} (\varphi_{1,N-1} - \varphi_{2,N-1} - \varphi_{e,N-1}) \right), \quad (14)
\end{aligned}$$

where  $k = 2, \dots, N-1$  and  $N$  is the number of SQUIDS in the array. Notice that this system contains  $2N$  equations for an array with  $N$  SQUIDS.

#### 4.2 Asymptotic solution without coupling

First, the average voltage response is numerically estimated for series coupled SQUID array without coupling ( $M = 0$ ). The equations for the series coupled SQUIDS,

where  $M = 0$ , can be written as

$$\begin{aligned}
\dot{\varphi}_{1,k} &= J - \frac{1}{\beta_k} (\varphi_{1,k} - \varphi_{2,k} - 2\pi\alpha_k x_e) - \sin \varphi_{1,k} \\
\dot{\varphi}_{2,k} &= J + \frac{1}{\beta_k} (\varphi_{1,k} - \varphi_{2,k} - 2\pi\alpha_k x_e) - \sin \varphi_{2,k}, \quad (15)
\end{aligned}$$

for  $k = 1, \dots, N$ . Let  $\Sigma_k = \frac{\varphi_{1,k} + \varphi_{2,k}}{2} = \theta_k + \frac{\pi}{2}$  and  $\delta_k = \varphi_{1,k} - \varphi_{2,k} - 2\pi\alpha_k x_e$ .

Recalling that  $\sin(A + \frac{\pi}{2}) = \cos A$  and  $\cos(A + \frac{\pi}{2}) = -\sin A$ , gives

$$\begin{aligned}
\dot{\theta}_k &= J - \cos \theta_k \cos \left( \frac{\delta_k + 2\pi\alpha_k x_e}{2} \right) \\
\dot{\delta}_k &= -\frac{2}{\beta_k} \delta_k + 2 \sin \theta_k \sin \left( \frac{\delta_k + 2\pi\alpha_k x_e}{2} \right).
\end{aligned}$$

These are exactly the same equations solved in the single SQUID case but now there are  $N$  of them. Thus, the asymptotic expansion for approximating  $\Sigma_{k,0}(\tau)$  and  $\delta_{k,0}(\tau)$  through the hybrid approach is:

$$\begin{aligned}
\Sigma_{k,0}(\tau) &= \theta_{k,0}(\tau) + \frac{\pi}{2} \\
&= 2 \tan^{-1} \left[ b_k^{-1} \tan \left( \frac{\phi_{k,0}(\tau)}{2} \right) \right] + \frac{\pi}{2} \\
\delta_{k,0}(\tau) &= K_k \frac{c_k \sin(\phi_{k,0}(\tau)) - \cos \phi_{k,0}(\tau)}{1 - a_{k,0} \cos \phi_{k,0}(\tau)}, \quad (16)
\end{aligned}$$

where

$$\begin{aligned}
b_k &= \sqrt{\frac{1 - a_{k,0}}{1 + a_{k,0}}}, \\
a_{k,0} &= -\frac{1}{J} \cos \left( \frac{\langle \delta_k \rangle + 2\pi\alpha_k x_e}{2} \right) \\
c_k &= \frac{2}{\beta_k \omega_{k,0}} \\
K_k &= \frac{2 \sin(\pi\alpha_k x_e)}{J(1 + c_k^2)} \\
\phi_{k,0}(\tau) &= (\omega_{k,0} + \Delta\omega_k)\tau \\
\omega_{k,0} &= J\sqrt{1 - a_{k,0}^2} \\
\Delta\omega_k &= \frac{\sin(\pi\alpha_k x_e)k \sqrt{1 - a_{k,0}^2} - 1}{2 a_{k,0}^2} + \frac{\cos(\pi\alpha_k x_e)K_k^2}{16} \\
&\quad \times \left( \frac{(a_{k,0}^2 - 2 - c_k^2(3a_{k,0}^2 - 2))\sqrt{1 - a_{k,0}^2}}{a_{k,0}^3(1 - a_{k,0}^2)} \right. \\
&\quad \left. - \frac{c_k^2(2a_{k,0}^4 - 4a_{k,0}^2 + 2) + 2 - 2a_{k,0}^2}{a_{k,0}^3(1 - a_{k,0}^2)} \right).
\end{aligned}$$

A comparison of the average voltage responses from simulating equation (15) and the analytical approximation in equation (16) is shown in Figure 12. The array has

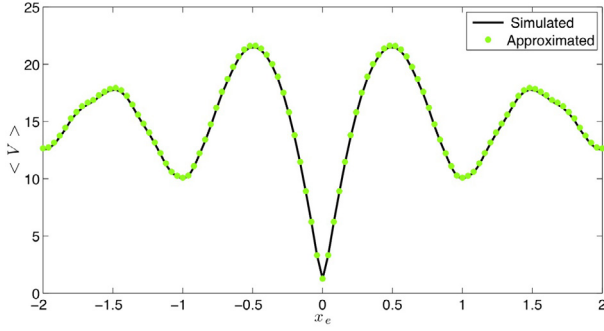


**Fig. 12.** Average voltage responses of the perturbation solution and the simulated solution of an array of 25 SQUIDs with a Gaussian distribution of  $\beta$  values between 0.5 and 1.5 with  $J = 1.001$ ,  $M = 0.0$  and  $x_e = [-2, 2]$ .

25 SQUIDs with a Gaussian distribution of  $\beta$  values in  $[0.5 : 1.5]$ . The simulations took 602.50 s to calculate the average voltage response and the analytical solution took 44.91 s, which is a speedup of 13.42. Visually the differences between the simulated and asymptotic solutions are minor. Calculation of the RMS error 0.013468 confirms this statement, since it is less than 25 times the error of the average voltage response of a single SQUID of size 1.0.

### 4.3 Asymptotic solution for nearest neighbor mutual inductance coupling

To get a more accurate asymptotic solution to the array of SQUIDs coupled in series the nearest neighbor mutual inductance coupling needs to be considered. A special case of equation (14) where  $N = 3$  is chosen in order to get insight into the complexity of the analysis, while keeping the number of terms more tractable for the complex perturbation mathematics. Recall that  $\Sigma_k = \frac{\varphi_{1,k} + \varphi_{2,k}}{2} = \theta_k + \frac{\pi}{2}$  and  $\delta_k = \varphi_{1,k} - \varphi_{2,k} - 2\pi\alpha_k x_e$  for  $k = 1, 2, 3$ . Time shift  $\bar{\tau} = J\tau$ , where  $\frac{d\theta_{k,0}}{d\bar{\tau}} = J\theta'_{k,0}$ , is performed on the  $\theta$  equations to yield

$$\begin{aligned}
 \theta'_1 &= 1 - \frac{1}{J} \cos \theta_1 \cos \left( \frac{\delta_1 + 2\pi\alpha_1 x_e}{2} \right) \\
 \dot{\delta}_1 &= -\frac{2}{\beta_1} \delta_1 + \frac{2M}{\beta_1\beta_2} \delta_2 + 2 \sin \theta_1 \sin \left( \frac{\delta_1 + 2\pi\alpha_1 x_e}{2} \right) \\
 \theta'_2 &= 1 - \frac{1}{J} \cos \theta_2 \cos \left( \frac{\delta_2 + 2\pi\alpha_2 x_e}{2} \right) \\
 \dot{\delta}_2 &= -\frac{2}{\beta_2} \delta_2 + \frac{2M}{\beta_2\beta_3} \delta_3 + \frac{2M}{\beta_1\beta_2} \delta_1 \\
 &\quad + 2 \sin \theta_2 \sin \left( \frac{\delta_2 + 2\pi\alpha_2 x_e}{2} \right) \\
 \theta'_3 &= 1 - \frac{1}{J} \cos \theta_3 \cos \left( \frac{\delta_3 + 2\pi\alpha_3 x_e}{2} \right) \\
 \dot{\delta}_3 &= -\frac{2}{\beta_3} \delta_3 + \frac{2M}{\beta_2\beta_3} \delta_2 + 2 \sin \theta_3 \sin \left( \frac{\delta_3 + 2\pi\alpha_3 x_e}{2} \right). \tag{17}
 \end{aligned}$$

An approximate solution to  $\theta_k$  and  $\delta_k$  are sought in the form:

$$\begin{aligned}
 \theta_k &= \theta_{k,0} + M\theta_{k,1} + \dots \\
 \delta_k &= \delta_{k,0} + M\delta_{k,1} + \dots, \tag{18}
 \end{aligned}$$

where  $M$  is the nearest neighbor mutual inductance coupling parameter. Substituting the asymptotic expansions in equation (18) into equation (17) and reorganizing the terms up to order  $\mathcal{O}(M^2)$  yields

$$\begin{aligned}
 \theta'_{1,0} + M\theta'_{1,1} &= 1 - \frac{1}{J} \cos(\theta_{1,0} + M\theta_{1,1}) \\
 &\quad \times \cos \left( \frac{\delta_{1,0}}{2} + \pi\alpha_1 x_e + \frac{M\delta_{1,1}}{2} \right) + \mathcal{O}(M^2) \\
 \dot{\delta}_{1,0} + M\dot{\delta}_{1,1} &= -\frac{2}{\beta_1} \delta_{1,0} - \frac{2M}{\beta_1} \delta_{1,1} + \frac{2M}{\beta_1\beta_2} \delta_{2,0} + \mathcal{O}(M^2) \\
 &\quad + 2 \sin(\theta_{1,0} + M\theta_{1,1}) \\
 &\quad \times \sin \left( \frac{\delta_{1,0}}{2} + \pi\alpha_1 x_e + \frac{M\delta_{1,1}}{2} \right) \\
 \theta'_{2,0} + M\theta'_{2,1} &= 1 - \frac{1}{J} \cos(\theta_{2,0} + M\theta_{2,1}) \\
 &\quad \times \cos \left( \frac{\delta_{2,0}}{2} + \pi\alpha_2 x_e + \frac{M\delta_{2,1}}{2} \right) + \mathcal{O}(M^2) \\
 \dot{\delta}_{2,0} + M\dot{\delta}_{2,1} &= -\frac{2}{\beta_2} \delta_{2,0} - \frac{2M}{\beta_2} \delta_{2,1} + \frac{2M}{\beta_2\beta_3} \delta_{3,0} \\
 &\quad + \frac{2M}{\beta_1\beta_2} \delta_{1,0} + 2 \sin(\theta_{2,0} + M\theta_{2,1}) \\
 &\quad \times \sin \left( \frac{\delta_{2,0}}{2} + \pi\alpha_2 x_e + \frac{M\delta_{2,1}}{2} \right) + \mathcal{O}(M^2) \\
 \theta'_{3,0} + M\theta'_{3,1} &= 1 - \frac{1}{J} \cos(\theta_{3,0} + M\theta_{3,1}) \\
 &\quad \times \cos \left( \frac{\delta_{3,0}}{2} + \pi\alpha_3 x_e + \frac{M\delta_{3,1}}{2} \right) + \mathcal{O}(M^2) \\
 \dot{\delta}_{3,0} + M\dot{\delta}_{3,1} &= -\frac{2}{\beta_3} \delta_{3,0} - \frac{2M}{\beta_3} \delta_{3,1} + \frac{2M}{\beta_2\beta_3} \delta_{2,0} + \mathcal{O}(M^2) \\
 &\quad + 2 \sin(\theta_{3,0} + M\theta_{3,1}) \\
 &\quad \times \sin \left( \frac{\delta_{3,0}}{2} + \pi\alpha_3 x_e + \frac{M\delta_{3,1}}{2} \right). \tag{19}
 \end{aligned}$$

Using Taylor expansions for cosine and sine and grouping like orders of  $\beta$ , then collecting the coefficients of like

powers of  $M$  gives the  $\mathcal{O}(M^0)$  equations

$$\begin{aligned}\theta'_{1,0} &= 1 - \frac{1}{J} \cos \theta_{1,0} \cos \left( \frac{\delta_{1,0}}{2} + \pi \alpha_1 x_e \right) \\ \dot{\delta}_{1,0} &= -\frac{2}{\beta_1} \delta_{1,0} + 2 \sin \theta_{1,0} \sin \left( \frac{\delta_{1,0}}{2} + \pi \alpha_1 x_e \right) \\ \theta'_{2,0} &= 1 - \frac{1}{J} \cos \theta_{2,0} \cos \left( \frac{\delta_{2,0}}{2} + \pi \alpha_2 x_e \right) \\ \dot{\delta}_{2,0} &= -\frac{2}{\beta_2} \delta_{2,0} + 2 \sin \theta_{2,0} \sin \left( \frac{\delta_{2,0}}{2} + \pi \alpha_2 x_e \right) \\ \theta'_{3,0} &= 1 - \frac{1}{J} \cos \theta_{3,0} \cos \left( \frac{\delta_{3,0}}{2} + \pi \alpha_3 x_e \right) \\ \dot{\delta}_{3,0} &= -\frac{2}{\beta_3} \delta_{3,0} + 2 \sin \theta_{3,0} \sin \left( \frac{\delta_{3,0}}{2} + \pi \alpha_3 x_e \right),\end{aligned}$$

and the  $\mathcal{O}(M^1)$  equations

$$\begin{aligned}\theta'_{1,1} &= \frac{1}{2J} \cos \theta_{1,0} \sin \left( \frac{\delta_{1,0}}{2} + \pi \alpha_1 x_e \right) \delta_{1,1} \\ &\quad + \frac{1}{J} \sin \theta_{1,0} \cos \left( \frac{\delta_{1,0}}{2} + \pi \alpha_1 x_e \right) \theta_{1,1} \\ \dot{\delta}_{1,1} &= -\frac{2}{\beta_1} \delta_{1,1} + \frac{2}{\beta_1 \beta_2} \delta_{2,0} \\ &\quad + \sin \theta_{1,0} \cos \left( \frac{\delta_{1,0}}{2} + \pi \alpha_1 x_e \right) \delta_{1,1} \\ &\quad + 2 \cos \theta_{1,0} \sin \left( \frac{\delta_{1,0}}{2} + \pi \alpha_1 x_e \right) \theta_{1,1} \\ \theta'_{2,1} &= \frac{1}{2J} \cos \theta_{2,0} \sin \left( \frac{\delta_{2,0}}{2} + \pi \alpha_2 x_e \right) \delta_{2,1} \\ &\quad + \frac{1}{J} \sin \theta_{2,0} \cos \left( \frac{\delta_{2,0}}{2} + \pi \alpha_2 x_e \right) \theta_{2,1} \\ \dot{\delta}_{2,1} &= -\frac{2}{\beta_2} \delta_{2,1} + \frac{2}{\beta_2 \beta_3} \delta_{3,0} + \frac{2}{\beta_1 \beta_2} \delta_{1,0} \\ &\quad + \sin \theta_{2,0} \cos \left( \frac{\delta_{2,0}}{2} + \pi \alpha_2 x_e \right) \delta_{2,1} \\ &\quad + 2 \cos \theta_{2,0} \sin \left( \frac{\delta_{2,0}}{2} + \pi \alpha_2 x_e \right) \theta_{2,1} \\ \theta'_{3,1} &= \frac{1}{2J} \cos \theta_{3,0} \sin \left( \frac{\delta_{3,0}}{2} + \pi \alpha_3 x_e \right) \delta_{3,1} \\ &\quad + \frac{1}{J} \sin \theta_{3,0} \cos \left( \frac{\delta_{3,0}}{2} + \pi \alpha_3 x_e \right) \theta_{3,1} \\ \dot{\delta}_{3,1} &= -\frac{2}{\beta_3} \delta_{3,1} + \frac{2}{\beta_2 \beta_3} \delta_{2,0} \\ &\quad + \sin \theta_{3,0} \cos \left( \frac{\delta_{3,0}}{2} + \pi \alpha_3 x_e \right) \delta_{3,1} \\ &\quad + 2 \cos \theta_{3,0} \sin \left( \frac{\delta_{3,0}}{2} + \pi \alpha_3 x_e \right) \theta_{3,1}.\end{aligned}$$

#### Perturbation solution

The  $\mathcal{O}(M^0)$  case is the series coupled SQUID arrays with no coupling term, which can be found in Section 4.2.

The solution to this case is

$$\begin{aligned}\theta_{k,0} &= \theta_{k,0,0} + \dots \\ \delta_{k,0} &= \delta_{k,0,0} + \dots\end{aligned}$$

where

$$\begin{aligned}\theta_{k,0,0}(\tau) &= 2 \tan^{-1} \left[ b_{k,0}^{-1} \tan \left( \frac{\phi_{k,0,0}(\tau)}{2} \right) \right] \\ \delta_{k,0,0}(\tau) &= K_{k,0} \frac{c_{k,0} \sin \phi_{k,0,0}(\tau) - \cos \phi_{k,0,0}(\tau)}{1 - a_{k,0,0} \cos \phi_{k,0,0}(\tau)},\end{aligned}\quad (20)$$

for  $k = 1, 2, 3$  with

$$\begin{aligned}b_{k,0} &= \sqrt{\frac{1 - a_{k,0,0}}{1 + a_{k,0,0}}} \\ a_{k,0,0} &= -\frac{1}{J} \cos \left( \frac{\langle \delta_{k,0} \rangle + 2\pi \alpha_k x_e}{2} \right) \\ c_{k,0} &= \frac{2}{\beta_k \omega_{k,0}} \\ K_{k,0} &= \frac{2 \sin(\pi \alpha_k x_e)}{J(1 + c_{k,0}^2)} \\ \phi_{k,0,0}(\tau) &= (\omega_{k,0,0} + \Delta \omega_{k,0}) \tau \\ \omega_{k,0,0} &= J \sqrt{1 - a_{k,0,0}^2} \\ \Delta \omega_{k,0} &= \frac{\sin(\pi \alpha_k x_e) k \sqrt{1 - a_{k,0,0}^2} - 1}{2 a_{k,0,0}^2} + \frac{\cos(\pi \alpha_k x_e) K_{k,0}^2}{16} \\ &\quad \times \left( \frac{(a_{k,0,0}^2 - 2 - c_{k,0}^2(3a_{k,0,0}^2 - 2)) \sqrt{1 - a_{k,0,0}^2}}{a_{k,0,0}^3(1 - a_{k,0,0}^2)} \right. \\ &\quad \left. - \frac{c_{k,0}^2(2a_{k,0,0}^4 - 4a_{k,0,0}^2 + 2) + 2 - 2a_{k,0,0}^2}{a_{k,0,0}^3(1 - a_{k,0,0}^2)} \right).\end{aligned}$$

Using the approximate solutions for  $\theta_{k,1}(\tau)$  and  $\delta_{k,1}(\tau)$  with the ten most dominant modes detailed in Appendix C, as well as  $\theta_{k,0}(\tau)$  and  $\delta_{k,0}(\tau)$  in equation (20), the final form for the system of equations can be written as:

$$\begin{aligned}\Sigma_k(\tau) &= \frac{\pi}{2} + \theta_{k,0}(\tau) + M \theta_{k,1}(\tau) \\ \delta_k(\tau) &= \delta_{k,0}(\tau) + M \delta_{k,1}(\tau),\end{aligned}\quad (21)$$

for  $k = 1, 2, 3$ . The solutions for  $\Sigma_k(\tau)$  and  $\delta_k(\tau)$  for three SQUIDS with  $M = 0.001$  are shown in Figure 13. The solid lines are simulations and the dashed lines are analytical solutions. The top plot is  $\Sigma_k(\tau)$  and the bottom plot is  $\delta_k(\tau)$ , bright green is  $k = 1$ , red is  $k = 2$  and blue is  $k = 3$ . The analytical solution is a decent approximation to the simulated results for small  $M$  with the green curves representing the solutions for the smallest value of  $\beta$  being the best approximations.

Figure 14 shows solutions for  $\Sigma_k(\tau)$  and  $\delta_k(\tau)$  for three SQUIDS with  $M = 0.1$ . The largest value for  $M$  that

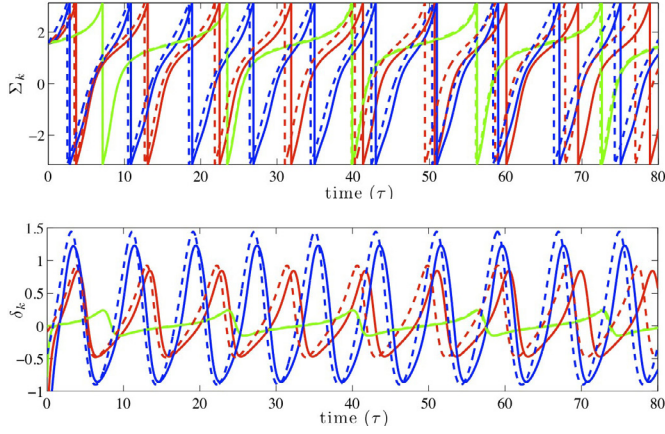


**Fig. 13.**  $\Sigma_k(\tau)$  (top) and  $\delta_k(\tau)$  (bottom) for  $k = 1$  (green),  $k = 2$  (red) and  $k = 3$  (blue) with  $M = 0.001$ ,  $x_e = [-2, 2]$ ,  $\beta = [0.5 \ 1.0 \ 1.5]$  and  $J = 1.001$ . The solid lines are simulations and the dashed lines are analytical solutions of a series coupled SQUID array.

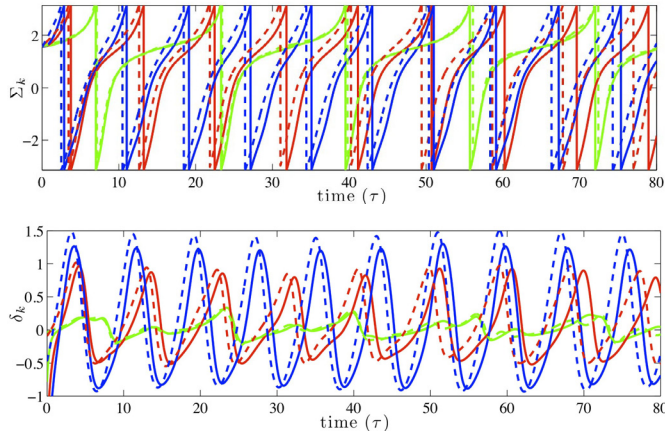


**Fig. 14.**  $\Sigma_k(\tau)$  (top) and  $\delta_k(\tau)$  (bottom) for  $k = 1$  (green),  $k = 2$  (red) and  $k = 3$  (blue) with  $M = 0.1$ ,  $x_e = [-2, 2]$ ,  $\beta = [0.5 \ 1.0 \ 1.5]$  and  $J = 1.001$ . The solid lines are simulations and the dashed lines are analytical solutions of a series coupled SQUID array.

our system can have is  $M_{max} = \beta_{min}$ . The derivation was calculated in the masters thesis of Aven [70]. In this situation  $\beta_{min} = 0.5$ , so  $M = 0.1$  is an acceptable value for the simulations. The solutions for  $\Sigma_k(\tau)$  do not line up as well as those for when  $M = 0.001$ , however the solutions for  $\delta_k(\tau)$  are about the same. This is probably owing to the solutions for  $\delta_{k,1}$  averaging near zero over time.

Using the same procedure to find numerical approximations for  $\Sigma_k(\tau)$  and  $\delta_k(\tau)$  for other values in  $x_e$  the average voltage response of the array of three SQUIDs can be calculated, see Figure 15. The solutions are obtained with the ten largest elements for the approximation of  $\theta_{k,1}(\tau)$  and  $\delta_{k,1}(\tau)$  with  $M = 0.001$ ,  $x_e = [-2, 2]$ ,  $\beta = [0.5 \ 1.0 \ 1.5]$  and  $J = 1.001$ . There is very strong correlation between the two solutions. It is our hope that this technique can

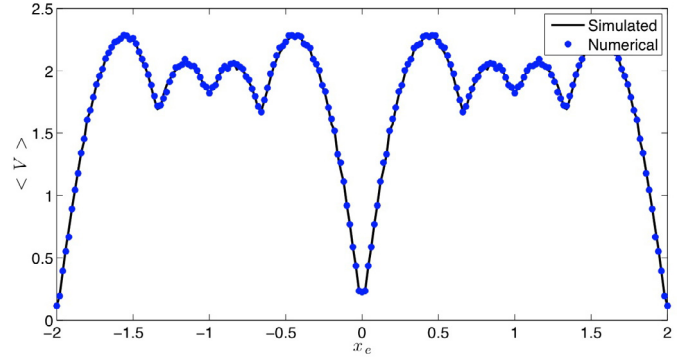


**Fig. 15.** Average voltage comparison for three SQUIDs, connected in series, where  $M = 0.001$ ,  $x_e = [-2, 2]$ ,  $\beta = [0.5 \ 1.0 \ 1.5]$  and  $J = 1.001$ .

be extended in future work to arrays of  $N > 3$  SQUIDs and for the bi-SQUID array equations.

## 5 Conclusion

In this paper we performed an extensive, analytical and computational, study of superconducting quantum interference devices (SQUIDs). While the basics of a single DC SQUID perturbation analysis had been demonstrated, an analysis like the one performed in this paper had not been done before. The results from the two approaches (straightforward and hybrid) to the perturbation analysis showed strong correlation between the simulated response and the numerical results for small values of  $\beta$ . For larger values of  $\beta$  the straightforward approach solution deteriorates while the hybrid approach, which represents the phase dynamics as non-uniform motion on a circle, continues to be an accurate approximation.

More specifically, for a single SQUID with values of  $\beta > 0.5$  and  $x_e \neq n$ , where  $n = 0, \pm 1, \pm 2, \dots$  the solutions of the straightforward approach have a much greater error than in the hybrid approach. The error progressively gets worse as  $\beta$  increases and  $x_e$  approaches  $n + \frac{1}{2}$ . This is true for  $J \geq 1$ , and every value of  $\alpha$  and  $\Sigma_0$  tested. For  $J < 1$  there are values of  $x_e$  for which the system is in the superconducting state. For these circumstances a different solution is needed, see work done by De Luca et al. [58]. On the other hand the hybrid approach is sufficiently accurate for any practical value of  $\beta$ ,  $\alpha$  and  $\Sigma_0$  when  $J \geq 1$ .

The hybrid approach was determined to result in a close analytical approximation for series coupled arrays of SQUIDs both uncoupled and with nearest neighbor mutual inductance coupling. Good comparisons were found for SQUID arrays with  $J \geq 1$ , all practical values attempted for  $\alpha$ ,  $\Sigma_0$ ,  $M$  and  $\beta_i$ , where  $i = 1, 2, \dots, N$  and  $N$  is the number of SQUIDs in the array. To continue this work the perturbation analysis needs to be extended to the parallel coupled DC SQUIDs as well as to DC bi-SQUID arrays. If accurate solutions are found, then the time consuming integrations of the governing equations

will no longer need to be performed, cutting down drastically on the time it takes to determine the average voltage response.

## Appendix A: Straightforward expansion details

This Appendix outlines the details of the straightforward perturbation analysis. The  $\mathcal{O}(\beta^0)$  and  $\mathcal{O}(\beta^1)$  systems of equations are

$$\begin{aligned}\frac{d\Sigma_0(\tau)}{d\tau} &= J - \sin \Sigma_0(\tau) \cos \delta_0(\nu) \\ \frac{d\delta_0(\nu)}{d\nu} &= -\delta_0(\nu) + \pi\alpha x_e,\end{aligned}\quad (\text{A.1})$$

and the  $\mathcal{O}(\beta^1)$  equations become

$$\begin{aligned}\frac{d\Sigma_1(\tau)}{d\tau} &= \sin \Sigma_0(\tau) \sin \delta_0(\nu) \delta_1(\nu) \\ &\quad - \cos \Sigma_0(\tau) \cos \delta_0(\nu) \Sigma_1(\tau) \\ \frac{d\delta_1(\nu)}{d\nu} &= -\delta_1(\nu) - \frac{1}{2} \sin \delta_0(\nu) \cos \Sigma_0(\tau).\end{aligned}\quad (\text{A.2})$$

### A.1 Solving the $\mathcal{O}(\beta^0)$ system

The second equation in equation (A.1) is solved first. Since  $\nu = \frac{2}{\beta}\tau$  it can be assumed that for small values of  $\beta$  the term  $\delta_0(\nu)$  is quasi-static in time or  $\frac{d\delta_0(\nu)}{d\nu} \approx 0$ , so

$$\delta_0(\nu) = \pi\alpha x_e.$$

Integrating the first equation in equation (A.1) yields

$$\begin{aligned}\tau + C &= \frac{1}{\sqrt{J^2 - \cos^2 \delta_0(\nu)}} \\ &\quad \times 2 \arctan \left( \frac{1}{2} \frac{2J \tan \left( \frac{1}{2} \Sigma_0(\tau) \right) - 2 \cos \delta_0(\nu)}{\sqrt{J^2 - \cos^2 \delta_0(\nu)}} \right),\end{aligned}$$

where  $\frac{1}{\left| \frac{\cos \delta_0(\nu)}{J} \right|} > 1$ . Solving for  $\Sigma_0(\tau)$  gives

$$\Sigma_0(\tau) = 2 \arctan \left( a + \sqrt{1 - a^2} \tan(\gamma\tau + \gamma C) \right),$$

where  $a = \frac{\cos \delta_0(\nu)}{J}$  and  $\gamma = \frac{1}{2} \sqrt{J^2 - \cos^2 \delta_0(\nu)}$ . Using the initial condition  $\Sigma_0(0)$  to solve for  $C$  yields

$$C = \frac{1}{\gamma} \arctan \left( \frac{\tan \left( \frac{1}{2} \Sigma_0(0) \right) - a}{\sqrt{1 - a^2}} \right).$$

The full solution is then written as:

$$\Sigma_0(\tau) = 2 \arctan \left( a + \sqrt{1 - a^2} \tan(\gamma\tau + \arctan(\xi_0)) \right),$$

where

$$a = \frac{\cos \delta_0(\nu)}{J}, \quad \gamma = \frac{1}{2} \sqrt{J^2 - \cos^2 \delta_0(\nu)}$$

and

$$\xi_0 = \frac{\tan \left( \frac{1}{2} \Sigma_0(0) \right) - a}{\sqrt{1 - a^2}}.$$

### A.2 Solving the $\mathcal{O}(\beta^1)$ system

The second equation in equation (A.2) is solved by assuming that  $\delta_1$  changes very slowly with respect to  $\nu$  so that

$$\delta_1(\nu) = -\frac{1}{2} \sin(\delta_0(\nu)) \cos \left( \Sigma_0 \left( \frac{\beta}{2} \nu \right) \right),$$

where  $\delta_0(\nu)$  and  $\Sigma_0(\frac{\beta}{2}\nu)$  have already been solved. Now the first equation in equation (A.2) is reorganized into the form of a standard ODE

$$\frac{d\Sigma_1(\tau)}{d\tau} + p(\tau)\Sigma_1(\tau) = q(\tau), \quad (\text{A.3})$$

where

$$\begin{aligned}p(\tau) &= \cos \Sigma_0(\tau) \cos \delta_0(\nu) \\ q(\tau) &= \sin \Sigma_0(\tau) \sin \delta_0(\nu) \delta_1(\nu).\end{aligned}$$

Equation (A.3) is solved using the integrating factor technique

$$\Sigma_1(\tau) = e^{-\int p(\tau) d\tau} \left[ \int e^{\int p(\tau) d\tau} q(\tau) d\tau + C \right]. \quad (\text{A.4})$$

Before jumping straight into the integration, some manipulation of  $p(\tau)$  and  $q(\tau)$  is needed. To start,  $p(\tau)$  can be written using the solutions to  $\Sigma_0(\tau)$  and  $\delta_0(\nu)$

$$\begin{aligned}p(\tau) &= \cos(\pi\alpha x_e) \cos \left( 2 \arctan \left( a + \sqrt{1 - a^2} \right. \right. \\ &\quad \left. \left. \times \tan(\gamma\tau + \arctan(\xi_0)) \right) \right).\end{aligned}$$

Using the double angle trigonometric identity for cosine gives

$$p(\tau) = \cos(2\theta) \cos(\pi\alpha x_e) = (\cos^2 \theta - \sin^2 \theta) \cos(\pi\alpha x_e),$$

with  $\theta = \arctan \left( a + \sqrt{1 - a^2} \tan(\gamma\tau + \arctan(\xi_0)) \right)$ . The trigonometric identity for tangent and the pythagorean theorem results in the identities

$$\begin{aligned}\cos \theta &= \frac{1}{\sqrt{1 + (a + \sqrt{1 - a^2} \tan(\gamma\tau + \arctan(\xi_0)))^2}} \\ \sin \theta &= \frac{a + \sqrt{1 - a^2} \tan(\gamma\tau + \arctan(\xi_0))}{\sqrt{1 + (a + \sqrt{1 - a^2} \tan(\gamma\tau + \arctan(\xi_0)))^2}}.\end{aligned}\quad (\text{A.5})$$

Using these identities,  $p(\tau)$  becomes

$$p(\tau) = \cos(\pi\alpha x_e) \times \frac{1 - (a + \sqrt{1 - a^2} \tan(\gamma\tau + \arctan(\xi_0)))^2}{1 + (a + \sqrt{1 - a^2} \tan(\gamma\tau + \arctan(\xi_0)))^2}. \quad (\text{A.6})$$

Similarly  $q(\tau)$  can be expanded by using the solutions to  $\Sigma_0(\tau)$ ,  $\delta_0(\nu)$  and  $\delta_1(\nu)$

$$q(\tau) = -\frac{1}{2} \sin^2(\pi\alpha x_e) \times \sin\left(2 \arctan\left(a + \sqrt{1 - a^2} \tan(\gamma\tau + \arctan(\xi_0))\right)\right) \times \cos\left(2 \arctan\left(a + \sqrt{1 - a^2} \tan(\gamma\tau + \arctan(\xi_0))\right)\right),$$

and by using the double angle trigonometric identities for cosine and sine results in

$$q(\tau) = -\sin^2(\pi\alpha x_e) \sin\theta \cos\theta (\cos^2\theta - \sin^2\theta),$$

where  $\theta = \arctan(a + \sqrt{1 - a^2} \tan(\gamma\tau + \arctan(\xi_0)))$ .

From equation (A.5)  $q(\tau)$  becomes

$$q(\tau) = -\sin^2(\pi\alpha x_e) \frac{\kappa(\tau) - \kappa(\tau)^3}{(1 + \kappa(\tau)^2)^2}, \quad (\text{A.7})$$

where  $\kappa(\tau) = a + \sqrt{1 - a^2} \tan(\gamma\tau + \arctan(\xi_0))$ .

Using equations (A.6) and (A.7) the terms  $e^{-\int p(\tau)d\tau}$  and  $e^{\int p(\tau)d\tau} q(\tau)$  are determined. First the integration of  $\int p(\tau)d\tau$  is performed

$$\int p(\tau)d\tau = \cos(\pi\alpha x_e) \frac{1}{2} \frac{1}{\sqrt{1 - a^2}\gamma a} \times \left( \ln(f_1)(a^2 - 1) + (1 - a^2) \ln(f_2) \right),$$

where

$$f_1 = \frac{1}{\cos(\gamma\tau + \arctan(\xi_0))^2}$$

$$f_2 = 2a^2 + \frac{2a\sqrt{1 - a^2} \sin(\gamma\tau + \arctan(\xi_0))}{\cos(\gamma\tau + \arctan(\xi_0))} + \frac{1 - a^2}{\cos^2(\gamma\tau + \arctan(\xi_0))}.$$

Next, the exponential  $e^{-\int p(\tau)d\tau}$  from equation (A.4) is manipulated. We use three steps:  $e^{x+y} = e^x e^y$ ,  $e^{a \ln(x)} = x^a$  then  $x^a y^{-a} = \left(\frac{x}{y}\right)^a$ . The result is the equation

$$e^{-\int p(\tau)d\tau} = \left(\frac{f_1}{f_2}\right)^{\frac{\sqrt{1 - a^2} \cos(\pi\alpha x_e)}{2\gamma a}}.$$

Using  $f_1$  and  $f_2$  the final form for  $e^{-\int p(\tau)d\tau}$  is:

$$\left(\frac{1}{2a^2 \cos \Gamma^2 + 2a\sqrt{A} \sin \Gamma \cos \Gamma + A}\right)^{\frac{\sqrt{A} \cos(\pi\alpha x_e)}{2\gamma a}}, \quad (\text{A.8})$$

where  $\Gamma = \gamma\tau + \arctan(\xi_0)$  and  $A = 1 - a^2$ . A similar equation is determined for  $e^{\int p(\tau)d\tau}$

$$\left(2a^2 \cos \Gamma^2 + 2a\sqrt{A} \sin \Gamma \cos \Gamma + A\right)^{\frac{\sqrt{A} \cos(\pi\alpha x_e)}{2\gamma a}}. \quad (\text{A.9})$$

Using equations (A.8), (A.9) and (A.7) and integrating equation (A.4), the solution to  $\Sigma_1(\tau)$  can be approximated as:

$$\Sigma_1(\tau) = \frac{8\pi \sin(\pi x_e)^2 \left(\tan(\Gamma) + a\sqrt{A} - a^3\sqrt{A}\right)}{\gamma a 4A(1 + a^2 + 2a\sqrt{A} \tan(\Gamma) + A \tan(\Gamma)^2)} + \frac{8\pi \sin(\pi x_e)^2 (-2 \arctan(\Gamma)a + a^4 \tan(\Gamma))}{\gamma a 4A(1 + a^2 + 2a\sqrt{A} \tan(\Gamma) + A \tan(\Gamma)^2)} - \frac{\pi \sin(\pi x_e)^2 \ln(1 + a^2 + 2a\sqrt{A} \tan(\Gamma))}{\gamma a^2 \sqrt{A}} - \frac{-a^2 \tan(\Gamma)^2 + \tan(\Gamma)^2 A}{\gamma a^2 \sqrt{A}} + \frac{\pi \sin(\pi x_e)^2 \sqrt{A} \ln(1 + \tan(\Gamma)^2)}{\gamma a^2} + C_0,$$

where

$$C_0 = e^{\int -p(\tau)d\tau} \left( \int e^{\int p(\tau)d\tau} q(\tau) d\tau \Big|_{\tau=0} \right)$$

$$\Gamma = \gamma\tau + \arctan(\xi_0)$$

$$A = 1 - a^2$$

$$a = \frac{\cos \delta_0(\nu)}{J}$$

$$\gamma = \frac{1}{2} \sqrt{J^2 - \cos^2 \delta_0(\nu)}$$

$$\xi_0 = \frac{\tan\left(\frac{1}{2} \Sigma_0(0)\right) - a}{\sqrt{1 - a^2}}.$$

The accuracy of the analytical approximation to  $\Sigma_1(\tau)$  is verified by comparison with numerical integration of

$$\frac{d\Sigma_1(\tau)}{d\tau} = \sin \Sigma_0(\tau) \sin \delta_0(\nu) \delta_1(\nu) - \cos \Sigma_0(\tau) \cos \delta_0(\nu) \Sigma_1(\tau).$$

The simulated solution and the numerical approximation shown in Figure A.1 appear to be identical to the naked eye and have  $\text{RMS} = 3.14961 \times 10^{-10} \approx 0$ , where the Root Mean Square (RMS) error is calculated

$$\text{RMS} = \frac{1}{N_T} \sqrt{\sum_{i=1}^{N_T} (\Sigma_{1,s}(i) - \Sigma_{1,a}(i))^2},$$

for which  $\Sigma_{1,s}$  is the simulated solution,  $\Sigma_{1,a}$  is the analytical approximation and  $N_T$  is the number of points in  $\tau$ .

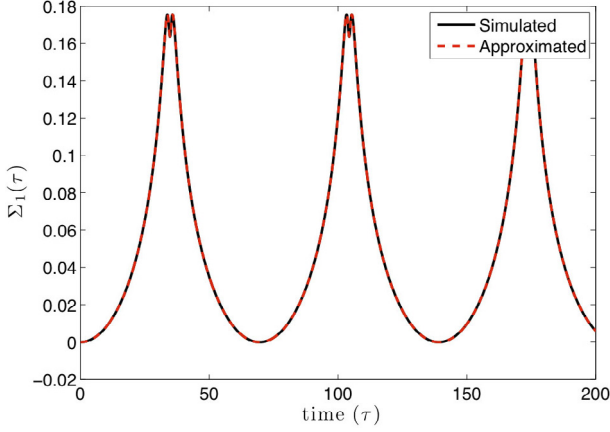


**Fig. A.1.** The simulated and numerical results for  $\Sigma_1(\tau)$  where  $x_e = 0.25$ ,  $\beta = \alpha = 0.1$ ,  $J = 1.001$ ,  $\Sigma(0) = \frac{\pi}{2}$ .

## Appendix B: Hybrid expansion details

This Appendix outlines the details of the hybrid perturbation analysis performed. The  $\mathcal{O}(\beta^0)$  system of equations is

$$\begin{aligned} \theta'_0 &= 1 + a_0 \cos \theta_0 \\ \dot{\delta}_0 &= -\frac{2}{\beta} \delta_0 + 2 \sin \theta_0 \sin \left( \frac{\delta_0 + 2\pi\alpha x_e}{2} \right). \end{aligned} \quad (\text{B.1})$$

### Solving the $\mathcal{O}(\varepsilon^0)$ system

A solution to  $\theta_0(\tau)$  is found by transforming the first equation in equation (B.1) to uniform rotation which angles through

$$\theta_0 \rightarrow \phi_0 \text{ with } \frac{d\phi_0}{d\bar{\tau}} = C,$$

where  $C$  is constant in time. Each side of this transformation can be written as:

$$\begin{aligned} 1 + a_0 \cos \theta_0 &= \frac{d\theta_0}{d\bar{\tau}} & \frac{d\phi_0}{d\bar{\tau}} &= C \\ d\bar{\tau} &= \frac{d\theta_0}{1 + a_0 \cos \theta_0} & d\bar{\tau} &= \frac{d\phi_0}{C}. \end{aligned}$$

Direct manipulation yields

$$\frac{d\theta_0}{1 + a_0 \cos \theta_0} = \frac{d\phi_0}{C}. \quad (\text{B.2})$$

The antenna technology suggests that  $a_0^2 > 1^2$ , so the integration of equation (B.2) over the period of oscillation is

$$\frac{2}{\sqrt{1 - a_0^2}} \tan^{-1} \left[ \sqrt{\frac{1 - a_0}{1 + a_0}} \tan \left( \frac{\theta_0}{2} \right) \right] \Big|_0^{2\pi} = \frac{2\pi}{C},$$

which reduces to

$$C = \sqrt{1 - a_0^2},$$

for uniform motion. An equation of  $\theta_0$  as a function of  $\phi_0$  is found by substituting  $C$  into equation (B.2) and reorganizing

$$d\phi_0 = \frac{\sqrt{1 - a_0^2}}{1 + a_0 \cos \theta_0} d\theta_0.$$

Integrating each side gives

$$\phi_0(\theta_0) = 2 \tan^{-1} \left[ b_0 \tan \left( \frac{\theta_0}{2} \right) \right],$$

where  $b_0 = \sqrt{\frac{1 - a_0}{1 + a_0}}$ . Reorganizing to get  $\theta_0$  as a function of  $\phi_0$  gives

$$\theta_0(\phi_0) = 2 \tan^{-1} \left[ b_0^{-1} \tan \left( \frac{\phi_0}{2} \right) \right].$$

To get  $\theta_0(\tau)$ , first  $\phi_0$  is solved as a function of  $\tau$

$$\phi_0(\tau) = C\bar{\tau} = J\sqrt{1 - a_0^2}\tau = \omega_0\tau,$$

where  $\omega_0 = J\sqrt{1 - a_0^2}$ . Then, the final equation for  $\theta_0(\tau)$  is:

$$\theta_0(\tau) = 2 \tan^{-1} \left[ b_0^{-1} \tan \left( \frac{\omega_0\tau}{2} \right) \right],$$

where  $b_0 = \sqrt{\frac{1 - a_0}{1 + a_0}}$ ,  $a_0 = -\frac{1}{J} \cos \left( \frac{\delta_0 + 2\pi\alpha x_e}{2} \right)$ , and  $\omega_0 = J\sqrt{1 - a_0^2}$ .

Next,  $\delta(\tau)$  is solved by considering the second equation in equation (B.1). Expanding  $\sin \left( \frac{\delta_0 + 2\pi\alpha x_e}{2} \right)$  using the angle sum sine trigonometric identity yields

$$\begin{aligned} \dot{\delta}_0 &= -\frac{2}{\beta} \delta_0 + 2 \sin \theta_0 \left[ \cos \left( \frac{\delta_0}{2} \right) \sin \left( \frac{2\pi\alpha x_e}{2} \right) \right. \\ &\quad \left. + \sin \left( \frac{\delta_0}{2} \right) \cos \left( \frac{2\pi\alpha x_e}{2} \right) \right]. \end{aligned}$$

Using Taylor series expansions for  $\cos \left( \frac{\delta_0}{2} \right)$  and  $\sin \left( \frac{\delta_0}{2} \right)$  and reducing  $\dot{\delta}_0$  to a first order ODE results in

$$\begin{aligned} \dot{\delta}_0 &= -\frac{2}{\beta} \delta_0 \\ &\quad + 2 \sin \theta_0 \left[ \sin(\pi\alpha x_e) + \frac{1}{2} \cos \left( \frac{2\pi\alpha x_e}{2} \right) \delta_0 \right]. \end{aligned} \quad (\text{B.3})$$

Using the identity  $\sin \theta_0 = \frac{\sqrt{1 - a_0^2} \sin(\omega_0\tau)}{1 - a_0 \cos(\omega_0\tau)}$ , equation (B.3) becomes

$$\begin{aligned} \dot{\delta}_0 &= -\frac{2}{\beta} \delta_0 \\ &\quad + \frac{2\sqrt{1 - a_0^2} \sin(\omega_0\tau)}{1 - a_0 \cos(\omega_0\tau)} \left[ \sin(\pi\alpha x_e) + \frac{1}{2} \delta_0 \cos(\pi\alpha x_e) \right]. \end{aligned} \quad (\text{B.4})$$

To integrate, equation (B.4) is reorganized into a standard form ODE

$$\frac{d\delta_0}{d\tau} + p(\tau)\delta_0 = q(\tau),$$

where the functions  $p(\tau)$  and  $q(\tau)$  are

$$p(\tau) = \frac{2}{\beta} - \frac{\sqrt{1-a_0^2} \cos(\pi\alpha x_e) \sin(\omega_0\tau)}{1-a_0 \cos(\omega_0\tau)}$$

$$q(\tau) = \frac{2\sqrt{1-a_0^2} \sin(\pi\alpha x_e) \sin(\omega_0\tau)}{1-a_0 \cos(\omega_0\tau)},$$

and which is solved using the integrating factor technique

$$\delta_0(\tau) = e^{-\int_0^\tau p(\tau)d\tau} \int_0^\tau e^{\int_0^\tau p(\tau)d\tau} q(\tau) d\tau.$$

Integration gives

$$\int p(\tau) d\tau = \frac{2}{\beta} \tau - \frac{\sqrt{1-a_0^2}}{a_0\omega_0} \cos(\pi\alpha x_e) \times \ln\left(\frac{1-a_0 \cos(\omega_0\tau)}{1-a_0}\right),$$

since  $\frac{\langle \delta \rangle}{2} \approx 0$  then  $\frac{\sqrt{1-a_0^2}}{a_0\omega_0} \cos(\pi\alpha x_e) = -1$ . This means that  $e^{-\int p(\tau)d\tau}$  and  $e^{\int p(\tau)d\tau}$  can be expressed as:

$$e^{-\int p(\tau)d\tau} = e^{-\frac{2}{\beta}\tau} e^{-\ln\left(\frac{1-a_0 \cos(\omega_0\tau)}{1-a_0}\right)}$$

$$= \frac{1-a_0}{1-a_0 \cos(\omega_0\tau)} e^{-\frac{2}{\beta}\tau}$$

$$e^{\int p(\tau)d\tau} = e^{\frac{2}{\beta}\tau} e^{\ln\left(\frac{1-a_0 \cos(\omega_0\tau)}{1-a_0}\right)}$$

$$= \frac{1-a_0 \cos(\omega_0\tau)}{1-a_0} e^{\frac{2}{\beta}\tau}. \quad (\text{B.5})$$

Using equation (B.5),  $\delta_0(\tau)$  becomes

$$\delta_0(\tau) = K \left( \frac{c \sin(\omega_0\tau) - \cos(\omega_0\tau)}{1-a_0 \cos(\omega_0\tau)} + \frac{e^{-\frac{2}{\beta}\tau}}{1-a_0 \cos(\omega_0\tau)} \right),$$

where  $K = \frac{2 \sin(\pi\alpha x_e)}{J(1+c^2)}$  and  $c = \frac{2}{\beta\omega_0}$ . To consider only the long-term behavior the limit is taken as  $\tau \rightarrow \infty$ , which gives the final solution for  $\delta_0(\tau)$

$$\lim_{\tau \rightarrow \infty} \delta_0(\tau) = \lim_{t \rightarrow \infty} \left\{ K \left[ \frac{c \sin(\omega_0\tau) - \cos(\omega_0\tau)}{1-a_0 \cos(\omega_0\tau)} + \frac{e^{-\frac{2}{\beta}\tau}}{1-a_0 \cos(\omega_0\tau)} \right] \right\}$$

$$= K \frac{c \sin(\omega_0\tau) - \cos(\omega_0\tau)}{1-a_0 \cos(\omega_0\tau)}.$$

To improve the results a first order frequency correction  $\Delta\omega$  can be found such that  $\phi(\tau) = \omega\tau$ , where  $\omega = \omega_0 + \Delta\omega$ . Recall that  $\frac{d\phi}{d\bar{\tau}} = \frac{\omega}{J}$ , so applying the Chain rule yields

$$\frac{\omega}{J} = \frac{d\phi}{d\bar{\tau}} = \frac{d\phi}{d\theta_0} \frac{d\theta_0}{d\bar{\tau}}.$$

From equations (B.2) and (11) and that  $\omega_0 = J\sqrt{1-a_0^2}$ ,  $\Delta\omega$  is solved to be

$$\Delta\omega = J \frac{\sqrt{1-a_0^2}}{1+a_0 \cos\theta_0} \varepsilon \cos\theta_0.$$

Using the trig identities  $\frac{1}{1+a_0 \cos\theta_0} = \frac{1-a_0 \cos\phi_0}{1-a_0^2}$  and  $\cos\theta_0 = \frac{\cos\phi_0 - a_0}{1-a_0 \cos\phi_0}$  then  $\Delta\omega$  can be rewritten as:

$$\Delta\omega = \frac{J}{\sqrt{1-a_0^2}} (a - a_0)(\cos\phi_0 - a_0).$$

To make  $\Delta\omega$  independent of  $\phi_0$  the average is performed over one period  $T = 2\pi$

$$\Delta\omega = \frac{J}{\sqrt{1-a_0^2}} \frac{1}{2\pi} \int_0^{2\pi} (\cos\phi_0 - a_0)(a(\phi_0) - a_0) d\phi_0. \quad (\text{B.6})$$

To solve for  $\Delta\omega$ ,  $a(\phi_0) = -\frac{1}{J} \cos\left(\frac{\delta_0(\phi_0)}{2}\right) + \pi\alpha x_e$  is expanded in a Taylor series about  $\pi\alpha x_e$  up to  $\mathcal{O}(\delta_0^2)$

$$a(\phi_0) = -\frac{\cos(\pi\alpha x_e)}{J} + \mathcal{O}(\delta_0^3)$$

$$+ \frac{1}{2} \frac{\sin(\pi\alpha x_e)}{J} K \frac{c \sin\phi_0 - \cos\phi_0}{1-a_0 \cos\phi_0} + \frac{K^2}{8}$$

$$\times \frac{\cos(\pi\alpha x_e) c^2 \sin^2\phi_0 - 2c \sin\phi_0 \cos\phi_0 + \cos^2\phi_0}{(1-a_0 \cos\phi_0)^2}. \quad (\text{B.7})$$

Substituting equation (B.7) into equation (B.6), performing the integrations and simplifying the correction to the frequency becomes

$$\Delta\omega = \frac{\sin(\pi\alpha x_e) K \sqrt{1-a_0^2} - 1}{2 a_0^2}$$

$$+ \frac{\cos(\pi\alpha x_e) K^2 (a_0^2 - 2 - c^2(3a_0^2 - 2)) \sqrt{1-a_0^2}}{16 a_0^3 (1-a_0^2)}$$

$$- \frac{\cos(\pi\alpha x_e) K^2 c^2 (2a_0^4 - 4a_0^2 + 2) + 2 - 2a_0^2}{16 a_0^3 (1-a_0^2)}.$$

## Appendix C: Coupled expansion details

This Appendix outlines the details of the perturbation analysis performed on a coupled system of three SQUIDs

with nearest neighbor mutual inductance coupling. The  $\mathcal{O}(\beta^1)$  system of equations is:

$$\begin{aligned}
\theta'_{1,1} &= \frac{1}{2J} \cos \theta_{1,0} \sin \left( \frac{\delta_{1,0}}{2} + \pi \alpha_1 x_e \right) \delta_{1,1} \\
&\quad + \frac{1}{J} \sin \theta_{1,0} \cos \left( \frac{\delta_{1,0}}{2} + \pi \alpha_1 x_e \right) \theta_{1,1} \\
\dot{\delta}_{1,1} &= -\frac{2}{\beta_1} \delta_{1,1} + \frac{2}{\beta_1 \beta_2} \delta_{2,0} \\
&\quad + \sin \theta_{1,0} \cos \left( \frac{\delta_{1,0}}{2} + \pi \alpha_1 x_e \right) \delta_{1,1} \\
&\quad + 2 \cos \theta_{1,0} \sin \left( \frac{\delta_{1,0}}{2} + \pi \alpha_1 x_e \right) \theta_{1,1} \\
\theta'_{2,1} &= \frac{1}{2J} \cos \theta_{2,0} \sin \left( \frac{\delta_{2,0}}{2} + \pi \alpha_2 x_e \right) \delta_{2,1} \\
&\quad + \frac{1}{J} \sin \theta_{2,0} \cos \left( \frac{\delta_{2,0}}{2} + \pi \alpha_2 x_e \right) \theta_{2,1} \\
\dot{\delta}_{2,1} &= -\frac{2}{\beta_2} \delta_{2,1} + \frac{2}{\beta_2 \beta_3} \delta_{3,0} + \frac{2}{\beta_1 \beta_2} \delta_{1,0} \\
&\quad + \sin \theta_{2,0} \cos \left( \frac{\delta_{2,0}}{2} + \pi \alpha_2 x_e \right) \delta_{2,1} \\
&\quad + 2 \cos \theta_{2,0} \sin \left( \frac{\delta_{2,0}}{2} + \pi \alpha_2 x_e \right) \theta_{2,1} \\
\theta'_{3,1} &= \frac{1}{2J} \cos \theta_{3,0} \sin \left( \frac{\delta_{3,0}}{2} + \pi \alpha_3 x_e \right) \delta_{3,1} \\
&\quad + \frac{1}{J} \sin \theta_{3,0} \cos \left( \frac{\delta_{3,0}}{2} + \pi \alpha_3 x_e \right) \theta_{3,1} \\
\dot{\delta}_{3,1} &= -\frac{2}{\beta_3} \delta_{3,1} + \frac{2}{\beta_2 \beta_3} \delta_{2,0} \\
&\quad + \sin \theta_{3,0} \cos \left( \frac{\delta_{3,0}}{2} + \pi \alpha_3 x_e \right) \delta_{3,1} \\
&\quad + 2 \cos \theta_{3,0} \sin \left( \frac{\delta_{3,0}}{2} + \pi \alpha_3 x_e \right) \theta_{3,1}.
\end{aligned}$$

### Solving the $\mathcal{O}(M^1)$ system

The  $\mathcal{O}(M^1)$  equations with the time shift  $\bar{\tau} = J\tau$  on the  $\theta$  equations are:

$$\begin{aligned}
\dot{\theta}_{1,1} &= A_1 \delta_{1,1} + B_1 \theta_{1,1} \\
\dot{\delta}_{1,1} &= P_1 + \left( -\frac{2}{\beta_1} + B_1 \right) \delta_{1,1} + 4A_1 \theta_{1,1} \\
\dot{\theta}_{2,1} &= A_2 \delta_{2,1} + B_2 \theta_{2,1} \\
\dot{\delta}_{2,1} &= P_2 + S_2 + \left( -\frac{2}{\beta_2} + B_2 \right) \delta_{2,1} + 4A_2 \theta_{2,1} \\
\dot{\theta}_{3,1} &= A_3 \delta_{3,1} + B_3 \theta_{3,1} \\
\dot{\delta}_{3,1} &= S_3 + \left( -\frac{2}{\beta_3} + B_3 \right) \delta_{3,1} + 4A_3 \theta_{3,1},
\end{aligned}$$

$$A_k = \frac{1}{2} \cos \theta_{k,0} \sin \left( \frac{\delta_{k,0} + 2\pi \alpha_k x_e}{2} \right)$$

$$B_k = \sin \theta_{k,0} \cos \left( \frac{\delta_{k,0} + 2\pi \alpha_k x_e}{2} \right)$$

$$P_k = \frac{2}{\beta_k \beta_{k+1}} \delta_{k+1,0}$$

$$S_k = \frac{2}{\beta_{k-1} \beta_k} \delta_{k-1,0}.$$

Substituting the solutions found for  $\theta_{k,0}$  and  $\delta_{k,0}$ ,  $A_k$  and  $B_k$  become, after some manipulation

$$\begin{aligned}
A_k &= \frac{1}{2} \frac{1 - \left( b^{-1} \tan \left( \frac{\Omega_{k,0}\tau}{2} \right) \right)^2}{1 + \left( b^{-1} \tan \left( \frac{\Omega_{k,0}\tau}{2} \right) \right)^2} \\
&\quad \times \left( \sin \left( \frac{K_{k,0} c_{k,0} \sin(\Omega_{k,0}\tau) - \cos(\Omega_{k,0}\tau)}{2(1 - a_{k,0,0} \cos(\Omega_{k,0}\tau))} \right) \right. \\
&\quad \times \cos(\pi \alpha_k x_e) \\
&\quad \left. + \cos \left( \frac{K_{k,0} c_{k,0} \sin(\Omega_{k,0}\tau) - \cos(\Omega_{k,0}\tau)}{2(1 - a_{k,0,0} \cos(\Omega_{k,0}\tau))} \right) \right. \\
&\quad \left. \times \sin(\pi \alpha_k x_e) \right) \\
B_k &= 2 \frac{b^{-1} \tan \left( \frac{\Omega_{k,0}\tau}{2} \right)}{1 + \left( b^{-1} \tan \left( \frac{\Omega_{k,0}\tau}{2} \right) \right)^2} \\
&\quad \times \left( \cos \left( \frac{K_{k,0} c_{k,0} \sin(\Omega_{k,0}\tau) - \cos(\Omega_{k,0}\tau)}{2(1 - a_{k,0,0} \cos(\Omega_{k,0}\tau))} \right) \right. \\
&\quad \times \cos(\pi \alpha_k x_e) \\
&\quad \left. - \sin \left( \frac{K_{k,0} c_{k,0} \sin(\Omega_{k,0}\tau) - \cos(\Omega_{k,0}\tau)}{2(1 - a_{k,0,0} \cos(\Omega_{k,0}\tau))} \right) \right. \\
&\quad \left. \times \sin(\pi \alpha_k x_e) \right)
\end{aligned}$$

where  $\Omega_{k,0} = \omega_{k,0,0} + \Delta\omega_{k,0}$  and  $b_{k,0}$ ,  $a_{k,0,0}$ ,  $c_{k,0}$ ,  $K_{k,0}$ ,  $\phi_{k,0,0}(\tau)$ ,  $\omega_{k,0,0}$  and  $\Delta\omega_{k,0}$  are the same as in the  $\mathcal{O}(M^0)$  system. Substituting  $\delta_{k+1,0}$  and  $\delta_{k-1,0}$  into  $P_k$  and  $S_k$ , respectively, gives:

$$P_k = \frac{2}{\beta_k \beta_{k+1}} K_{k+1,0} \frac{c_{k+1,0} \sin(\Omega_{k+1,0}\tau) - \cos(\Omega_{k+1,0}\tau)}{1 - a_{k+1,0,0} \cos(\Omega_{k+1,0}\tau)}$$

$$S_k = \frac{2}{\beta_{k-1} \beta_k} K_{k-1,0} \frac{c_{k-1,0} \sin(\Omega_{k-1,0}\tau) - \cos(\Omega_{k-1,0}\tau)}{1 - a_{k-1,0,0} \cos(\Omega_{k-1,0}\tau)}.$$

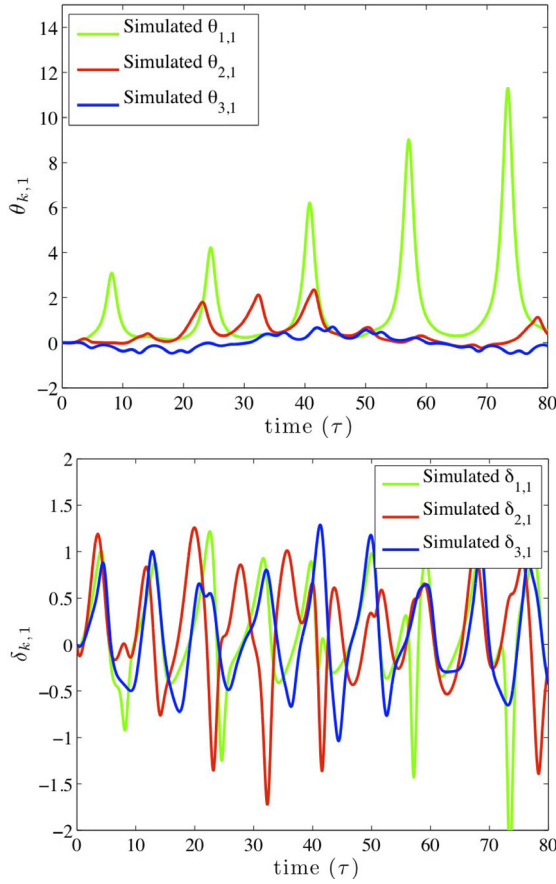


**Fig. C.1.** Simulated solutions  $\theta_{k,1}(\tau)$  (top) and  $\delta_{k,1}(\tau)$  (bottom),  $k = 1, 2, 3$ , for  $\beta = [0.5 \ 1.0 \ 1.5]$ ,  $x_e = 0.25$  and  $J = 1.001$ .

Integrating the equations for  $\dot{\theta}_{k,1}$  and  $\dot{\delta}_{k,1}$ ,  $k = 1, 2, 3$ , gives the time response shown in Figure C.1. On the left-hand side is  $\theta_{k,1}(\tau)$  and on the right-hand side is  $\delta_{k,1}(\tau)$ . For these simulations,  $\beta_1 = 0.5$ ,  $\beta_2 = 1.0$ ,  $\beta_3 = 1.5$ ,  $x_e = 0.25$  and  $J = 1.001$ . The dynamics cannot be reconstructed by a simple function but rather a compilation of many of cosine and sine functions might be needed. To approximate these solutions a summation of sines and cosines can be created using the frequencies present in a power spectral density (PSD) of the simulated solutions.

Figure C.2 shows the PSD for  $\theta_{1,1}(\tau)$  on the top and  $\delta_{1,1}(\tau)$  on the bottom. The PSD is calculated using a Fast Fourier Transform (FFT) using the Matlab function `fft` and is represented as  $\theta_{1,1}(f) = FFT(\theta_{1,1}(\tau))$  and  $\delta_{1,1}(f) = FFT(\delta_{1,1}(\tau))$ . Similar plots were made for  $\theta_{2,1}(\tau)$ ,  $\theta_{3,1}(\tau)$ ,  $\delta_{2,1}(\tau)$  and  $\delta_{3,1}(\tau)$ . The solid lines represent the energy obtained from the FFT of the simulations of the differential equations of  $\theta_{1,1}(\tau)$  and  $\delta_{1,1}(\tau)$ . The black dots represent the ten largest frequency contributions to the dynamics of  $\theta_{1,1}(\tau)$  and  $\delta_{1,1}(\tau)$ , which are related to the most dominant cosine and sine modes. Finally, the dashed lines are the PSD from the approximations of  $\theta_{1,1}(\tau)$  and  $\delta_{1,1}(\tau)$  using the ten largest frequency contributions.

Using the ten dominant frequencies from the PSD, approximate equations for  $\theta_{1,1}(\tau)$  and  $\delta_{1,1}(\tau)$  can be found

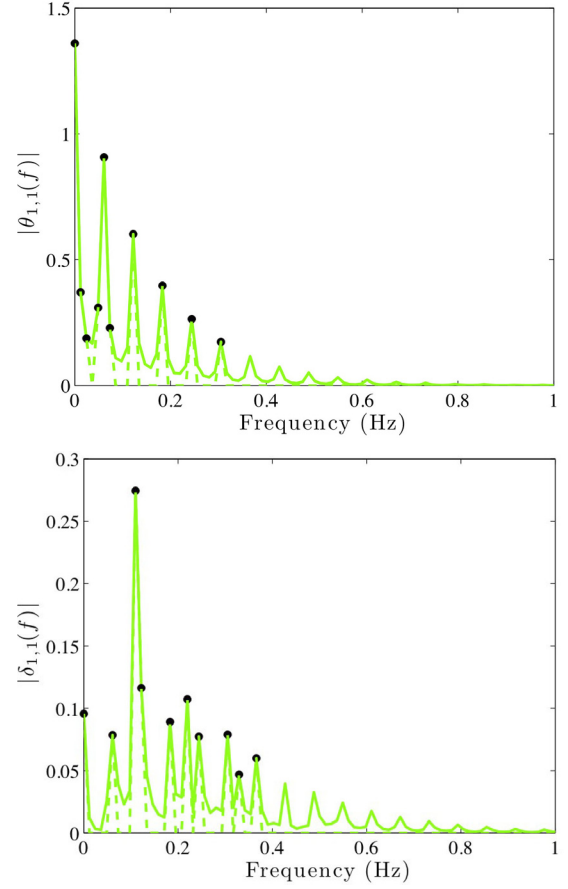


**Fig. C.2.** PSD for  $\theta_{1,1}(\tau)$  on the top and  $\delta_{1,1}(\tau)$  on the bottom. The solid lines are the PSD from the simulations, the black dots are the 10 largest frequency contributions and the dashed lines are the PSD from the approximations of  $\theta_{1,1}(\tau)$  and  $\delta_{1,1}(\tau)$  using the 10 largest frequency contributions.

as a summation of cosines and sines. The variables  $\theta_{2,1}$ ,  $\theta_{3,1}$ ,  $\delta_{2,1}$  and  $\delta_{3,1}$  are determined in a similar fashion, but are not expressed explicitly for brevity. The approximate equations for  $\theta_{1,1}(\tau)$  are:

$$\begin{aligned} \theta_{1,1} = & 1.35965 - 1.80654 \cos(2\pi 0.06104\tau) \\ & + 0.16089 \sin(2\pi 0.06104\tau) + 1.18016 \cos(2\pi 0.12207\tau) \\ & - 0.23745 \sin(2\pi 0.12207\tau) - 0.76945 \cos(2\pi 0.18311\tau) \\ & + 0.19376 \sin(2\pi 0.18311\tau) + 0.07409 \cos(2\pi 0.01221\tau) \\ & - 0.73652 \sin(2\pi 0.01221\tau) - 0.18301 \cos(2\pi 0.04883\tau) \\ & - 0.59082 \sin(2\pi 0.04883\tau) + 0.49808 \cos(2\pi 0.24414\tau) \\ & - 0.17565 \sin(2\pi 0.24414\tau) + 0.02975 \cos(2\pi 0.07324\tau) \\ & + 0.45600 \sin(2\pi 0.07324\tau) - 0.02099 \cos(2\pi 0.02441\tau) \\ & - 0.37402 \sin(2\pi 0.02441\tau) - 0.32097 \cos(2\pi 0.30517\tau) \\ & + 0.12903 \sin(2\pi 0.30516\tau), \end{aligned}$$

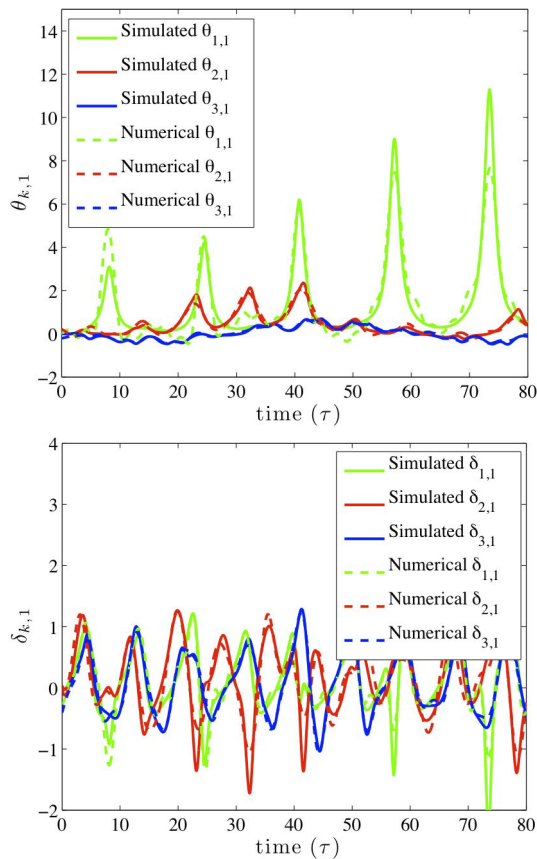


**Fig. C.3.** Simulated results (solid lines) for  $\theta_{k,1}$  (top) and  $\delta_{k,1}$  (bottom),  $k = 1, 2, 3$ , compared with the approximated results (dotted lines) with the top 10 largest contributions where  $\beta = [0.5 \ 1.0 \ 1.5]$ ,  $x_e = 0.25$  and  $J = 1.001$ .

and for  $\delta_{1,1}(\tau)$  are:

$$\begin{aligned} \delta_{1,1} = & 0.09565 - 0.46271 \cos(2\pi \cdot 0.10986\tau) \\ & + 0.29572 \sin(2\pi \cdot 0.10986\tau) - 0.23259 \cos(2\pi \cdot 0.12207\tau) \\ & + 0.00450 \sin(2\pi \cdot 0.12207\tau) + 0.20171 \cos(2\pi \cdot 0.21973\tau) \\ & - 0.07327 \sin(2\pi \cdot 0.21973\tau) + 0.17799 \cos(2\pi \cdot 0.18311\tau) \\ & + 0.00985 \sin(2\pi \cdot 0.18311\tau) + 0.15682 \cos(2\pi \cdot 0.30518\tau) \\ & - 0.01827 \sin(2\pi \cdot 0.30518\tau) + 0.15388 \cos(2\pi \cdot 0.06104\tau) \\ & + 0.03191 \sin(2\pi \cdot 0.06104\tau) - 0.15438 \cos(2\pi \cdot 0.24414\tau) \\ & + 0.00983 \sin(2\pi \cdot 0.24414\tau) - 0.11733 \cos(2\pi \cdot 0.36621\tau) \\ & + 0.02565 \sin(2\pi \cdot 0.36621\tau) - 0.08875 \cos(2\pi \cdot 0.32959\tau) \\ & - 0.02995 \sin(2\pi \cdot 0.32959\tau). \end{aligned}$$

When the simulated results for  $\theta_{k,1}$  and  $\delta_{k,1}$ ,  $k = 1, 2, 3$ , are plotted against the approximated results (obtained with the ten most dominant frequency components) the results are shown in Figure C.3. In this plot  $\theta_{k,1}$  are on the top and  $\delta_{k,1}$  are on the bottom. The solid lines are

the results from the simulations and the dotted lines are the results from the approximations. For these simulations  $\beta_1 = 0.5$ ,  $\beta_2 = 1.0$ ,  $\beta_3 = 1.5$ ,  $x_e = 0.25$  and  $J = 1.001$ . The results from the approximations with ten frequencies are significantly close to the results from the simulations. If the number of elements in the approximation is increased, the simulated and approximated solutions become more alike. For a very large number of elements, for instance the top 100 frequency contributions, the two plots are almost identical.

## References

1. C.J. Poole, *Handbook of Superconductivity* (Academic Press, 2000)
2. J. Clarke, *Scientific American* **271**, 46 (1994)
3. D.V. Delft, P. Kes, J. Overweg, J. Zaanen, in *100 Years of Superconductivity, Leiden, 8 April 2011*
4. R. Kleiner, D. Koelle, F. Ludwig, J. Clarke, *Proc. IEEE* **92**, 1534 (2004)
5. R.C. Jaklevic, J. Lambe, A.H. Silver, J.E. Mercereau, *Phys. Rev. Lett.* **12**, 159 (1964)
6. F. London, *Superfluids* (Wiley, New York, 1950)
7. B. Deaver Jr., W. Fairbank, *Phys. Rev. Lett.* **7**, 43 (1961)
8. R. Doll, M. Nöbauer, *Phys. Rev. Lett.* **7**, 51 (1961)
9. *100 Years of Superconductivity*, edited by H. Rogalla, P. Kes (CRC Press, 2012)
10. R.L. Fagaly, *Rev. Sci. Instrum.* **77**, 101101 (2006)
11. L.E. Fong, J.R. Holzer, K.K. McBride, E.A. Lima, F. Baudenbacher, M. Radparvar, *Rev. Sci. Instrum.* **76**, 053703 (2005)
12. O. Hahnseier, S. Kohlsmann, M. Hetscher, K.D. Kramer, *Bioelectrochemistry and Bioenergetics* **37**, 51 (1995)
13. Y. Machitani, N. Kasai, Y. Fujinawa, H. Iitaka, N. Shirai, Y. Hatsukade, K. Nomura, K. Sugiura, A. Ishiyama, T. Nemoto, *IEEE Trans. Appl. Supercond.* **13**, 763 (2003)
14. P. Schmidt, D. Clark, K.E. Leslie, M. Bick, D.L. Tilbrook, C.P. Foley, *Exploration Geophysics* **35**, 297 (2004)
15. A. Chwala, R. Stolz, R. IJsselsteijn, F. Bauer, V. Zakosarenko, U. Hubner, H. Meyer, M. Meyer, *SEG Technical Program Expanded Abstracts* **29**, 779 (2010)
16. M. Espy, S. Baguisa, D. Dunkerley, P. Magnelind, A. Matlashov, T. Owens, H. Sandin, I. Savukov, L. Schultz, A. Urbaitis, P. Volegov, *IEEE Trans. Appl. Supercond.* **21**, 530 (2011)
17. R. Bradley, J. Clarke, D. Kinion, L. Rosenberg, K. van Bibber, S. Matsuki, M. Mueck, P. Sikivie, *Rev. Mod. Phys.* **75**, 777 (2003)
18. D.G. Aronson, M. Golubitsky, M. Krupa, *Nonlinearity* **4**, 861 (1991)
19. M. Inchiosa, A. Bulsara, K. Wiesenfeld, L. Gammaitoni, *Phys. Lett. A* **252**, 20 (1999)
20. M. Inchiosa, V. In, A. Bulsara, K. Wiesenfeld, T. Heath, M. Choi, *Phys. Rev. E* **63**, 1 (2001)
21. A. Bulsara, A.K.V. In, P. Longhini, A. Palacios, W. Rappel, J. Acebron, S. Baglio, B. Ando, *Phys. Rev. E* **70**, 036103 (2004)
22. A. Palacios, J. Aven, P. Longhini, V. In, A. Bulsara, *Phys. Rev. E* **74**, 021122 (2006)
23. K. Stawiasz, M. Ketchen, *IEEE Trans. Appl. Supercond.* **3**, 1808 (1993)

24. J. Oppenländer, Ch. Häussler, N. Schopohl, Phys. Rev. B **63**, 024511 (2000)
25. C. Häussler, J. Oppenländer, N. Schopohl, J. Appl. Phys. **89**, 1875 (2001)
26. T. Träuble, J. Oppenländer, C. Häussler, N. Schopohl, Physica C **368**, 119 (2002)
27. J. Oppenländer, C. Häussler, T. Träuble, P. Caputo, J. Tomes, A. Friesch, N. Schopohl, IEEE Trans. Appl. Supercond. **13**, 771 (2003)
28. J. Oppenländer, T. Träuble, C. Häussler, N. Schopohl, IEEE Trans. Appl. Supercond. **11**, 1271 (2001)
29. J. Oppenländer, C. Häussler, A. Friesch, J. Tomes, P. Caputo, T. Träuble, N. Schopohl, IEEE Trans. Appl. Supercond. **15**, 936 (2005)
30. V.K. Kornev, I.I. Soloviev, N.V. Klenov, O.A. Mukhanov, IEEE Trans. Appl. Supercond. **19**, 741 (2009)
31. V.K. Kornev, I.I. Soloviev, J. Oppenländer, C. Häussler, N. Schopohl, Supercond. Sci. Technol. **17**, S406 (2004)
32. V. Schultze, R. IJsselsteijn, H.G. Meyer, J. Oppenländer, C. Häussler, N. Schopohl, IEEE Trans. Appl. Supercond. **13**, 775 (2003)
33. V. Schultze, R. IJsselsteijn, H.G. Meyer, Supercond. Sci. Technol. **19**, S411 (2006)
34. J. Oppenländer, P. Caputo, C. Häussler, T. Träuble, J. Tomes, A. Friesch, N. Schopohl, Appl. Phys. Lett. **83**, 969 (2003)
35. P. Caputo, J. Oppenländer, C. Häussler, J. Tomes, A. Friesch, T. Träuble, N. Schopohl, Appl. Phys. Lett. **85**, 1389 (2004)
36. P. Caputo, J. Tomes, J. Oppenländer, C. Häussler, A. Friesch, T. Träuble, N. Schopohl, IEEE Trans. Appl. Supercond. **15**, 1044 (2005)
37. Y. Polyakov, V. Semenov, S. Tolpygo, IEEE Trans. Appl. Supercond. **21**, 724 (2011)
38. P. Caputo, J. Tomes, J. Oppenländer, C. Häussler, A. Friesch, T. Träuble, N. Schopohl, IEEE Trans. Appl. Supercond. **17**, 722 (2006)
39. V.K. Kornev, I.I. Soloviev, N.V. Klenov, T. Filippov, H. Engseth, O.A. Mukhanov, IEEE Trans. Appl. Supercond. **19**, 916 (2009)
40. V.K. Kornev, I.I. Soloviev, N.V. Klenov, A.V. Sharafiev, O.A. Mukhanov, IEEE Trans. Appl. Supercond. **21**, 713 (2011)
41. P. Caputo, J. Tomes, J. Oppenländer, C. Häussler, A. Friesch, T. Träuble, N. Schopohl, Appl. Phys. Lett. **89**, 062507 (2006)
42. P. Caputo, J. Tomes, J. Oppenländer, Ch. Häussler, A. Friesch, T. Träuble, N. Schopohl, J. Supercond. Novel Magn. **20**, 25 (2007)
43. A. Shadrin, K. Constantinian, G. Ovsyannikov, Tech. Phys. Lett. **33**, 192 (2007)
44. A.K. Kalabukhov, M.L. Chukharkin, A.A. Deleniv, D. Winkler, I.A. Volkov, O.V. Snigirev, J. Commun. Technol. Electron. **53**, 934 (2008)
45. V.K. Kornev, I.I. Soloviev, N.V. Klenov, A.V. Sharafiev, O.A. Mukhanov, Physica C **479**, 119 (2012)
46. K. Wiesenfeld, A. Bulsara, M. Inghisa, Phys. Rev. B **62**, R9232 (2000)
47. M. Mück, R. McDermott, Supercond. Sci. Technol. **23**, 093001 (2010)
48. C. Hilbert, J. Clarke, J. Low Temp. Phys. **61**, 263 (1985)
49. M. Cyrille, Thin Solid Films **333**, 228 (1998)
50. O. Snigirev, M. Chukharkin, A. Kalabukhov, M. Tarasov, A.A. Deleniv, O.A. Mukhanov, D. Winkler, IEEE Trans. Appl. Supercond. **17**, 718 (2007)
51. V.K. Kornev, I.I. Soloviev, N.V. Klenov, O.A. Mukhanov, IEEE Trans. Appl. Supercond. **17**, 569 (2007)
52. J. Luine, L. Abelson, D. Brundrett, J. Burch, E. Dantsker, K. Hummer, G. Kerber, M. Wire, K. Yokoyama, D. Bowling, M. Neel, S. Hubbell, K. Li, IEEE Trans. Appl. Supercond. **9**, 4141 (1999)
53. A.M.L. Martin, D.R. Bowling, M.M. Neel, Naval Eng. J. **110**, 123 (1998)
54. S.K. Khamas, M.J. Mehler, T.S.M. Maclean, C.E. Gough, Electron. Lett. **24**, 460 (1988)
55. K. Sakuta, Y. Narita, H. Itozaki, Supercond. Sci. Technol. **20**, S389 (2007)
56. T. Lanting, M. Dobbs, H. Spieler, A.T. Lee, Y. Yamamoto, arXiv:0901.1919 [astro-ph.IM] (2009)
57. J. Beyer, D. Drung, Supercond. Sci. Technol. **21**, 095012 (2008)
58. R. De Luca, A. Fedullo, V. Gasanenko, Eur. Phys. J. B **58**, 461 (2007)
59. S. Yukon, DTIC Online (2010), pp. 1–25
60. F. Romeo, R.D. Luca, Phys. Lett. A **328**, 330 (2004)
61. N. Grønbech-Jensen, C. Cosmelli, D. Thompson, M. Cirillo, Phys. Rev. B **67**, 224505 (2003)
62. K. Tsang, R. Mirolo, S. Strogatz, K. Wiesenfeld, Physica D **48**, 102 (1991)
63. M. Bennett, K. Wiesenfeld, Physica D **192**, 196 (2004)
64. K. Wiesenfeld, J. Swift, Phys. Rev. E **51**, 1020 (1995)
65. S. Watanabe, S. Strogatz, Physica D **74**, 197 (1994)
66. J. Swift, S. Strogatz, K. Wiesenfeld, Physica D **55**, 239 (1992)
67. S. Watanabe, J. Swift, J. Nonlinear Sci. **7**, 503 (1997)
68. A. Barone, G. Paterno, *Physics and Applications of the Josephson Effect* (J. Wiley, New York, 1982)
69. A. Bulsara, J. Acebron, W. Rappel, A. Hibbs, L. Kunstmanas, M. Krupka, Physica A **325**, 220 (2003)
70. J.L. Aven, Networks of coupled SQUID magnetometers, Master's thesis, San Diego State University, 2006